Int. J. Dev. Biol. 41: 425-447 (1997)

Original Article

Role of the retinoic acid receptor beta (RARβ) during mouse development

NORBERT B. GHYSELINCK, VALÉRIE DUPÉ, ANDRÉE DIERICH, NADIA MESSADDEQ, JEAN-MARIE GARNIER, CÉCILE ROCHETTE-EGLY, PIERRE CHAMBON and MANUEL MARK*

Institut de Génétique et de Biologie Moléculaire et Cellulaire, CNRS/INSERM/ULP, Collège de France, Strasbourg, France

ABSTRACT Homozygous RARβ mutants are growth-deficient, but are fertile and have a normal longevity. They display homeotic transformations and malformations of cervical vertebrae and a retrolenticular membrane. This latter abnormality arises from the persistence and hyperplasia of the primary vitreous body. In contrast, we found that abnormalities of cranial nerves IX and X which were previously proposed to be specific features of the RARβ mutant phenotype (Luo *et al., Mech. Dev. 53:* 61-71, 1995) occur with the same low penetrance in wildtype littermates. Although the RARβ protein is expressed at high levels in the striatum and interdigital mesenchyme, the brain and limbs of RARβ mutants appear morphologically normal. RARα/RARβ double mutants display numerous visceral abnormalities, most of which are incompatible with post-natal life. The majority of these abnormalities was previously detected in RARα/RARβ2 mutants with the notable exceptions of agenesis of the stapedial (2nd aortic arch-derived) artery, thymic and spleen agenesis and abnormal inferior vena cava. RARβ/RARγ double mutants show major ocular defects including a shortening of the ventral retina and pre-natal retinal dysplasia, both of which represent the only abnormalities of the fetal vitamin-A deficiency (VAD) syndrome not previously detected in RARβ2/RARγ compound mutants. In addition, RARβ is apparently functionally redundant with either RARα or RARγ for the formation of a small subset of craniofacial skeletal elements, as well as for eyelid development and digit separation. We also provide evidence that, at least in some instances, this phenomenon of functional redundancy between RARs may be an artifactual consequence of gene knock-out.

KEY WORDS: *retinoic acid receptors, morphogenesis, gene knockout, mouse embryonic development, genetic redundancy*

Introduction

Retinoids, the biologically active derivatives of vitamin A, have been implicated in many aspects of vertebrate physiology and homeostasis (Wolbach and Howe, 1925; Blomhoff, 1994; Underwood and Arthur 1996 for reviews and references). In addition, they appear to play essential roles in organogenesis, as inferred from the large spectrum of developmental abnormalities displayed by vitamin A deficient (VAD) fetuses (reviewed in Wilson *et al.*, 1953). During the past decade, the characterization of two families of nuclear receptors for retinoids, the RARs (RARα, β, and γ; activated by all natural forms retinoic acids – RA) and the RXR (RXRα, β and γ; activated only by 9-cis RA) has revealed the complexity of the molecular machinery transducing the retinoid signal. An additional level of complexity was brought to light by the finding that RXRs not only form homodimers, but can also heterodimerize with a variety of other nuclear receptors. Most notably, it was demonstrated that RXRs represent the nuclear factors required by RARs to bind tightly to a variety of cognate response elements *in vitro* and to transactivate in transfected cells (Mangelsdorf and Evans, 1995; Chambon, 1996, and references therein). Furthermore, a clear convergence between the RXRα and RAR signaling pathways has been revealed in cultured cells and in the mouse (Kastner *et al.*, 1995 and 1997; Chambon, 1996, and references therein).

Genetic analysis of the functions of the various RARs in the mouse has clearly shown that they mediate the developmental functions of retinoids since, altogether, RARβ2 single null mutants (Mendelsohn *et al.*, 1994c; Grondona *et al.*, 1996), RARα1$^{-/-}$/RARβ2$^{-/-}$, RARα$^{-/-}$/RARβ2$^{-/-}$, RARβ2$^{-/-}$/RARγ$^{-/-}$, RARα$^{-/-}$/RARγ$^{-/-}$ and RARα1$^{-/-}$/RARβ$^{-/-}$ double mutants (Lohnes *et al.*, 1994; Mendelsohn *et al.*, 1994b; Luo *et al.*, 1996) recapitulated almost all of the VAD-induced developmental defects (i.e. the fetal VAD syndrome). In addition to establishing the involvement of RA and

Abbreviations used in this paper: LBD, ligand binding domain; NCC, neural crest cells; PHPV, persistent hyperplastic primary vitreous; RA, retinoic acid, RAR and RXR are retinoic acid receptors; VAD, vitamin A deficiency; WT, wildtype.

***Address for reprints:** Institut de Génétique et de Biologie Moléculaire et Cellulaire, CNRS/INSERM/ULP, BP 163, 67404 Illkirch Cedex, France. FAX: +33.388653202. e-mail: igbmc@igbmc.u-strasbg.fr

0214-6282/97/$05.00

Printed in Spain

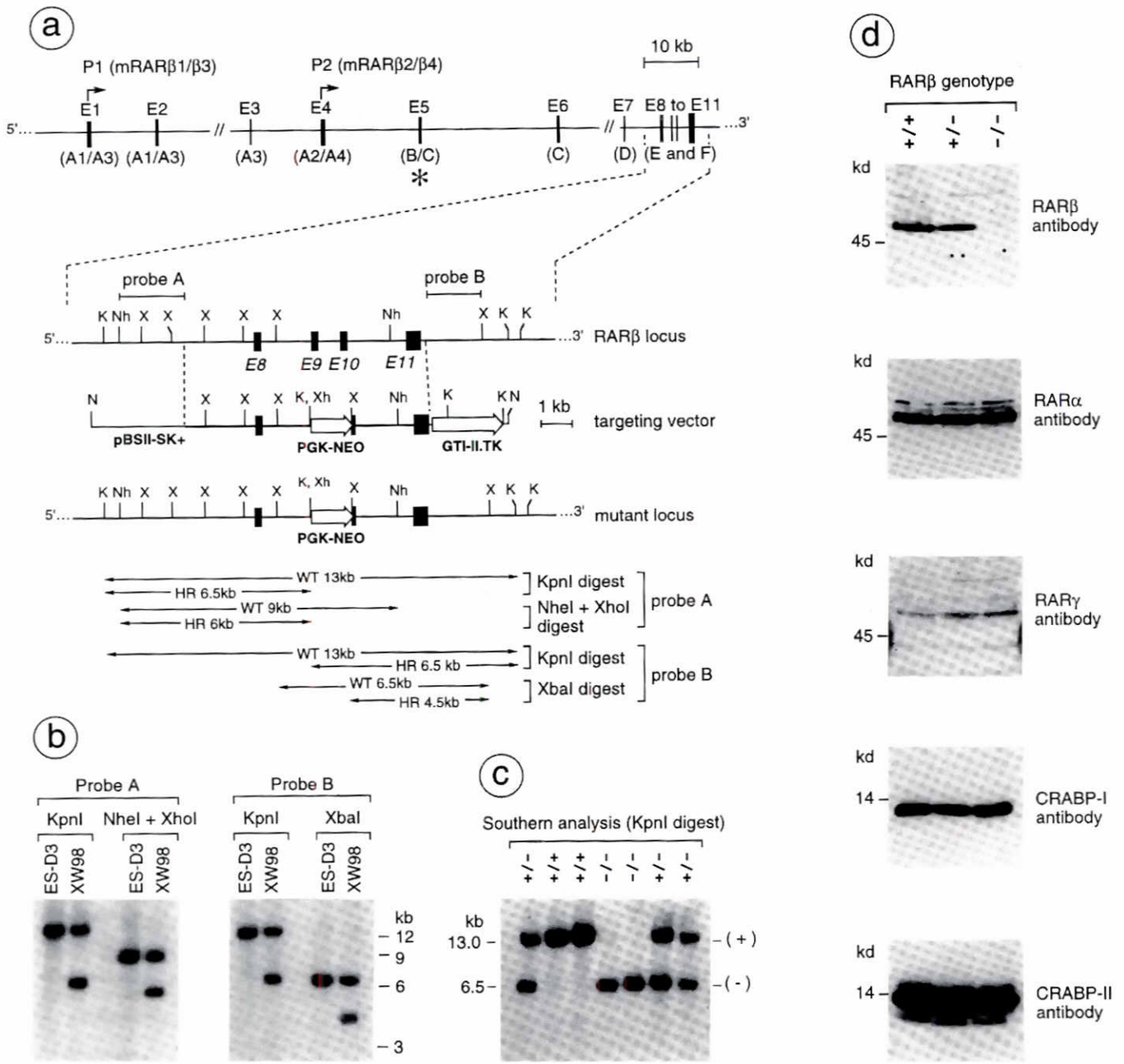

Fig. 1. Targeted disruption of the RARβ gene. (a) *A schematic drawing of the RARβ locus is shown at the top. The eleven exons are presented as solid boxes on the genomic DNA. As indicated below the exons, E1 to E4 are specific for RARβ isoforms, while E5 to E11 are used to compose the B to F region of all four isoforms. The alternative promoters (P1 and P2) are indicated by broken arrows. The asterisk points to the exon mutated by Luo et al. (1995). The enlargement represents exons E8 to E11 containing the ligand binding domain common to all isoforms. The RARβ targeting vector and the expected structure of the recombinant mutant allele are shown at the bottom. The predicted genomic fragments detected with the probes following KpnI, NheI-XhoI or XbaI digestion are indicated for both the wild type (WT) and the recombinant allele (HR). Restriction sites are: K, KpnI; N, NotI; Nh, NheI; X, XbaI; Xh, XhoI.* **(b)** *Genomic DNA from D3 ES cells and targeted ES cells (XW98) were digested with KpnI, NheI-XhoI or XbaI, as indicated, blotted and hybridized with the 5' external probe (probe A, left side) or the 3' external probe (probe B, right side). DNA size is indicated to the left of the figure in kilobases (kb).* **(c)** *Southern blot of DNA derived from 2-week-old offspring of heterozygous RARβ$^{+/-}$ intercrosses showing the presence of homozygous (-/-, containing the 6.5 kb KpnI fragment only), heterozygous (+/-, containing both the 6.5 and 13.0 kb KpnI fragments) and wild type (+/+, containing the 13 kb KpnI fragment only) alleles.* **(d)** *Western blot analysis showing expression of RARβ, RARα, RARγ, CRABP-I and CRABP-II in RARβ mutant. About 80 μg of nuclear extracts or 20 μg of cytosolic extracts from E10.5 WT (+/+), RARβ heterozygous (+/-) and RARβ homozygous (-/-) embryos were subjected to SDS-PAGE and immunostaining. The nuclear extracts were immunoprobed with the RARβ specific antiserum. Note the absence of the 55 kDa RARβ signal in the mutant embryo. After stripping, the same blot was subsequently probed with the RARα and the RARγ specific antisera. The hazy bands upper from the RARγ-specific band is a nonspecific signal and is independent of the RARβ genotype. The cytosolic extracts were first probed with the CRABP-I monoclonal antibody and then with the CRABP-II monoclonal antibody.*

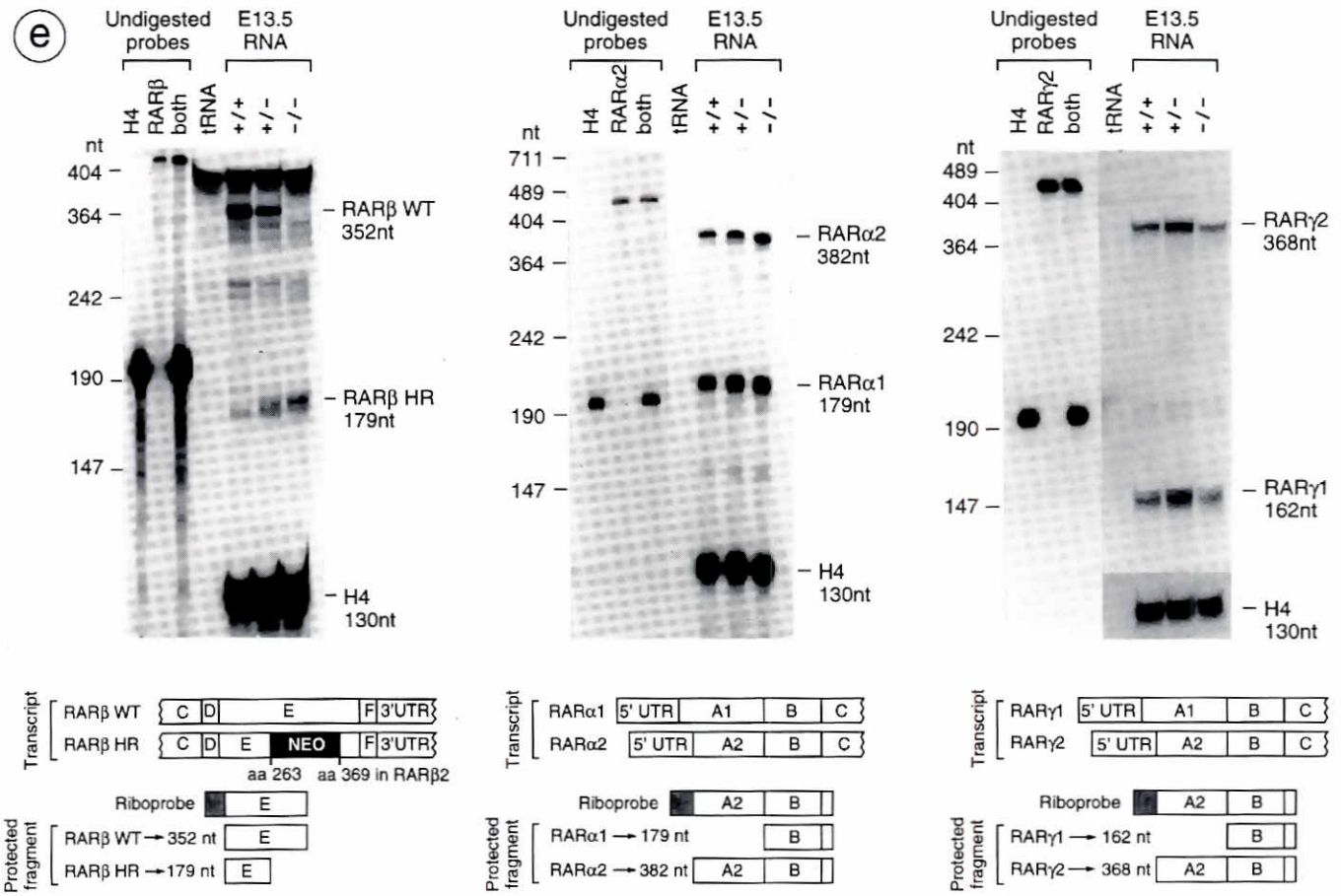

Fig. 1. Targeted disruption of the RARβ gene. (e) *RNAse protection analysis showing RARβ (left panel), RARα (middle panel) and RARγ (right panel) transcripts in E13.5 WT (+/+), heterozygous (+/-) and homozygous (-/-) embryos for RARβ disruption. The representation of the strategy for RNAse protection analysis, with the probes used and the expected protected fragments, is illustrated in the lower part of the figure. RARβ wildtype transcripts are represented at the top of the diagram, with the predicted RARβ mutated transcripts shown immediately below. Neo indicates the position of the neomycin resistance gene (not to scale), resulting from targeting of the cognate allele. The amino acid numbers delineating the deletion are relative to the RARβ2 isoform. The riboprobe used is shown in the middle of the diagram, followed by the protected fragments for both wildtype (WT) and mutated (HR) RARβ RNA, as indicated on the left. In each case the identity of the protected fragments with their size are indicated to the right of the gel. A tRNA sample was used as negative control and the histone H4 (probe is a gift of R. Grosschedl) protection was included as an internal control for the quantitation and integrity of the RNA samples. Note that the increase in RARγ levels is artifactual since H4 RNA levels are also increased in this experiment.*

RARs in the known functions of vitamin A during organogenesis, the analysis of RAR-deficient mice has revealed numerous abnormalities that had not previously been associated with an impaired vitamin A function, most notably neural tube defects, vertebral homeotic transformations, cranial and limb skeletal deficiencies and glandular abnormalities (reviewed in Kastner *et al.*, 1995).

In the case of the RARβ isotype, four isoforms (RARβ1 to RARβ4) have been characterized, each exhibiting a specific expression pattern in adult tissues (Zelent *et al.*, 1991; Nagpal *et al.*, 1992). The distribution of RARβ isoforms in embryonic tissues has not been analyzed, although differential activity of the two RARβ promoters was reported (Mendelsohn *et al.*, 1991, 1994a). Nevertheless, *in situ* hybridization data suggested that RARβ could play unique roles in the differentiation of the tracheal, intestinal and genital tract epithelia, as well as in the ontogenesis of the limbs and nervous system (Dollé *et al.*, 1990; Ruberte *et al.*, 1991). Previous analyses of mice lacking either the RARβ2 and β4 isoforms or all RARβ isoforms (RARβ 'total') revealed only two types of abnormalities: a mass of pigmented tissue behind the lens (retrolenticular membrane) observed only in RARβ2/β4 mutants (Grondona *et al.*, 1996), and a fusion of cranial nerves IX and X observed only in RARβ 'total' mutants (Luo *et al.*, 1995). With the aim of understanding these apparent discrepancies between the two phenotypes and to uncover the possible specific function(s) of the RARβ1 and β3 isoforms, we have now generated our own mice lacking all RARβ isoforms. Our analysis indicates that RARβ 'total' mutants indeed display a retrolenticular membrane and that this abnormality represents a congenital defect. Additionally, our RARβ mutants are growth-deficient and exhibit vertebral homeotic transformations. In contrast, abnormalities of cranial nerves IX and X do not appear to be specific features of the RARβ 'total' mutant phenotype. We also report the congenital defects observed by introduc-

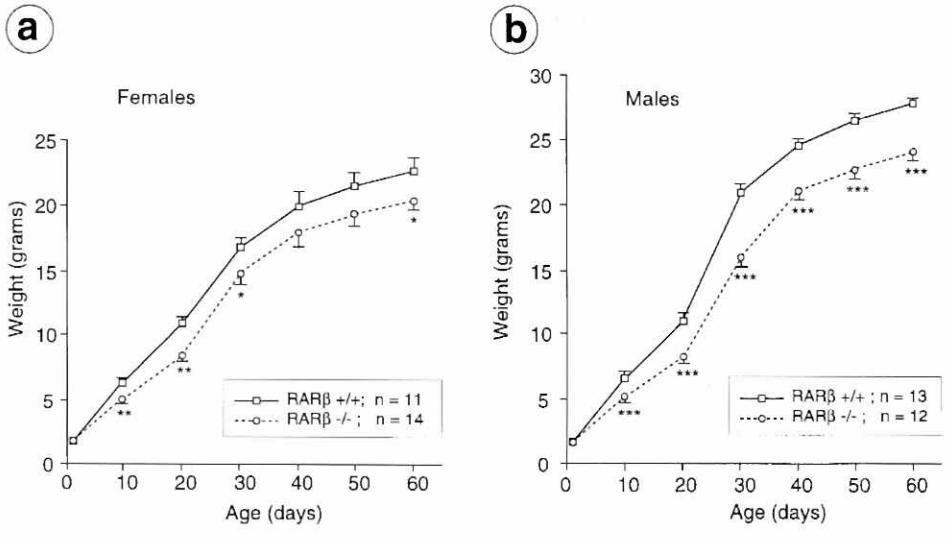

Fig. 2. Weight of female (a) and male (b) mice wildtype (+/+) and homozygous (-/-) for the RARβ null mutation. *Offspring (130) derived from intercrosses between RARβ$^{+/-}$ mice were weighed every 10 days from birth until 2 months of age. The numbers of animals in each group is indicated. Means of weights are presented with standard errors. After testing for normality and variance homogeneity, results obtained for unpaired values were subjected to Student's t test between group of mice for each genotype. The 0.05 level was selected as the point of minimal statistic significance. Asterisks indicate the level of significance for the observed differences between +/+ and -/- mice (*p<0.05; **p<0.01 and ***p<0.001).*

ing the RARβ 'total' mutation in RARα or RARγ null genetic backgrounds.

Results

Targeted disruption of the RARβ gene

Genomic clones were isolated from a genomic DNA library derived from the 129/Sv strain. Exon mapping of these clones showed that the RARβ gene extended over 120kb (Fig. 1a, top) and that its exonic organization was similar to that of the human RARβ gene (van der Leede *et al.*, 1992). Although we successfully disrupted the RARβ2 isoform at exon E4 in ES cells without too much difficulty (Mendelsohn *et al.*, 1994c), the disruption of the RARβ gene (all isoforms) proved to be much more difficult. We had to 'move along' the RARβ gene before finding a region which could be targeted. For unknown reasons, several attempts to target at the level of exon E5 (B domain of RARβ) and exon E6 (C domain of RARβ) were unsuccessful in our hands. In contrast, Luo *et al.* (1995) succeeded in disrupting the RARβ gene by replacing exon E5 (asterisk in Fig. 1a) by a neomycin resistance gene (Neo). We finally isolated one ES cell clone exhibiting a targeted RARβ allele at the level of exons E9 and E10. The replacement-type targeting vector (Capecchi, 1989) used to obtain this clone contains about 7kb of mouse genomic DNA in which the sequences encoding the ligand binding domain (LBD – common to all RARβ isoforms), between amino acids number 263 and 369 (numbering of the RARβ2 isoform), were replaced with a Neo cassette (Fig. 1a, bottom). The resulting protein should be truncated in helix H5 of the LBD just prior to isoleucine 263, one of the specific ligand-binding pocket residues (Renaud *et al.*, 1995). This deletion, encompassing most of the LBD and the entire F region, was shown to completely abolish both the ligand-inducible transactivation functions of RARβ (Folkers *et al.*, 1993; N.G. and P.C., unpublished results), the dimerization properties and the binding to a RA-response element (N.G. and P.C., data not shown). The linearized targeting vector was electroporated into D3 ES cells and 1 targeted clone out of 130 colonies was identified by Southern blot analysis using a probe (probe A) located immediately 5' to the replacement construct (Fig. 1b). The structure of the targeted allele was further characterized in this clone (XW98). DNA was digested with several enzymes and hybridized with either the 5' or a 3' probe (probe B). Duplications or rearrangements were not detected (Fig. 1b). In addition, Southern blots hybridized with a Neo probe showed the pattern expected for a single targeting event, indicating that no non-homologous recombination event had occurred in this ES cells line (data not shown). The clone XW98 was injected into C57BL/6 blastocysts to create chimeric mice, out of which 4 males transmitted the mutation to their offspring (Fig. 1c).

Western blot analysis was used to verify that the RARβ gene was functionally disrupted. Antibodies directed against the F region common to all RARβ isoforms readily detected the receptor in extracts from 10.5 day post-coitum (i.e. embryonic day 10.5: E10.5) wildtype (WT) and heterozygous embryos, whereas no receptor was detected in RARβ mutant homozygotes (Fig 1d). Immunoblotting with antibodies directed against RARα, RARγ, CRABPI and CRABPII (Fig. 1d) did not reveal any significant variation (within the sensitivity of the assay) among the same protein extracts. RNAse protection assays were also carried out using RNA from E13.5 fetuses (a time at which RARβ RNA is abundantly expressed, Zelent *et al.*, 1991). WT and heterozygous embryos for the RARβ mutation expressed the RARβ RNA as evidenced by the 352 nt long protected fragment (RARβ WT, Fig. 1e, left panel). Additionally, the heterozygous embryos expressed

TABLE 1

VIABILITY AND FERTILITY OF RARβ MUTANT MICE

Intercrosses	Genotype of offspring		
	+/+	+/-	-/-
Male Aβ+/- x Female Aβ+/-	44 (1.0)	110 (2.5)	52 (1.2)
Male Aβ x Female Aβ+/-	-	30 (1.0)	35 (1.2)
Male Aβ+/- x Female Aβ	-	35 (1.0)	33 (0.9)

The number of wild type offspring was arbitrarily assigned a value of 1.0 and the relative ratio of heterozygote and homozygote animals was calculated accordingly (numbers in parentheses).

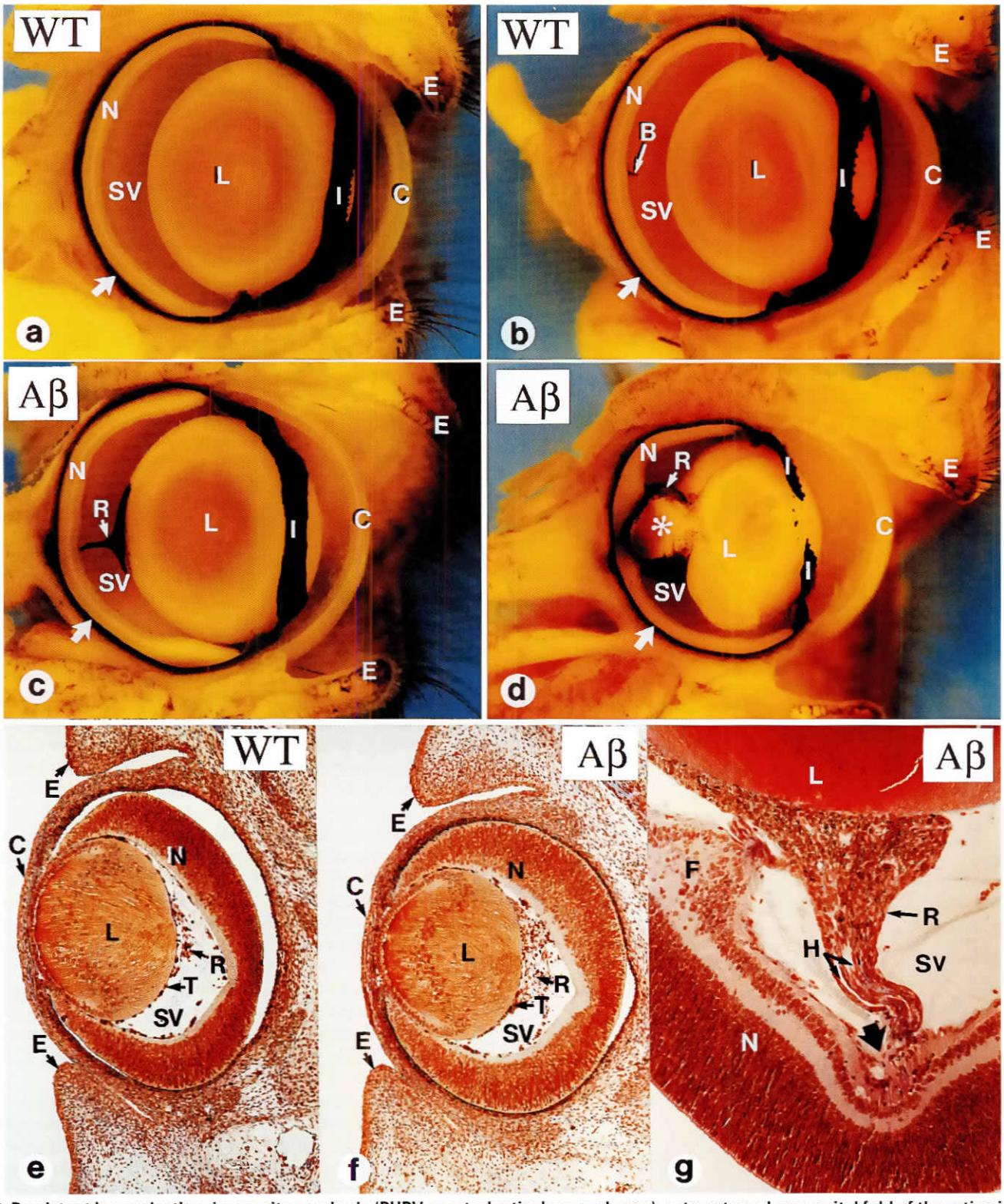

Fig. 3. Persistent hyperplastic primary vitreous body (PHPV or retrolenticular membrane), cataracts and congenital fold of the retina in Aβ null mutants. (a-d) *Comparison of adult (6 months old) WT and Aβ mutant eyes.* **(e,f)** *Comparison of frontal histological sections from E14.5 WT and Aβ mutant eyes.* **(g)** *Histological section through the PHPV at P4. B, Bergmeister's papilla; C, cornea; E, eyelids; F, congenital retinal fold; H, hyaloid artery and vein; I, iris; L, lens; N, neural retina; R, primary vitreous body (E14.5) or retrolenticular membrane (P4 and adults); SV, secondary vitreous body; T, vascular capsule of the lens. The large white arrow points to the choroid and retinal pigment epithelium which are indistinguishable from one another on macroscopical specimens. The large black arrow points toward the optic papilla. The asterisk indicates the cataract. Same magnifications in a-d; e,f: x70; and g: x140.*

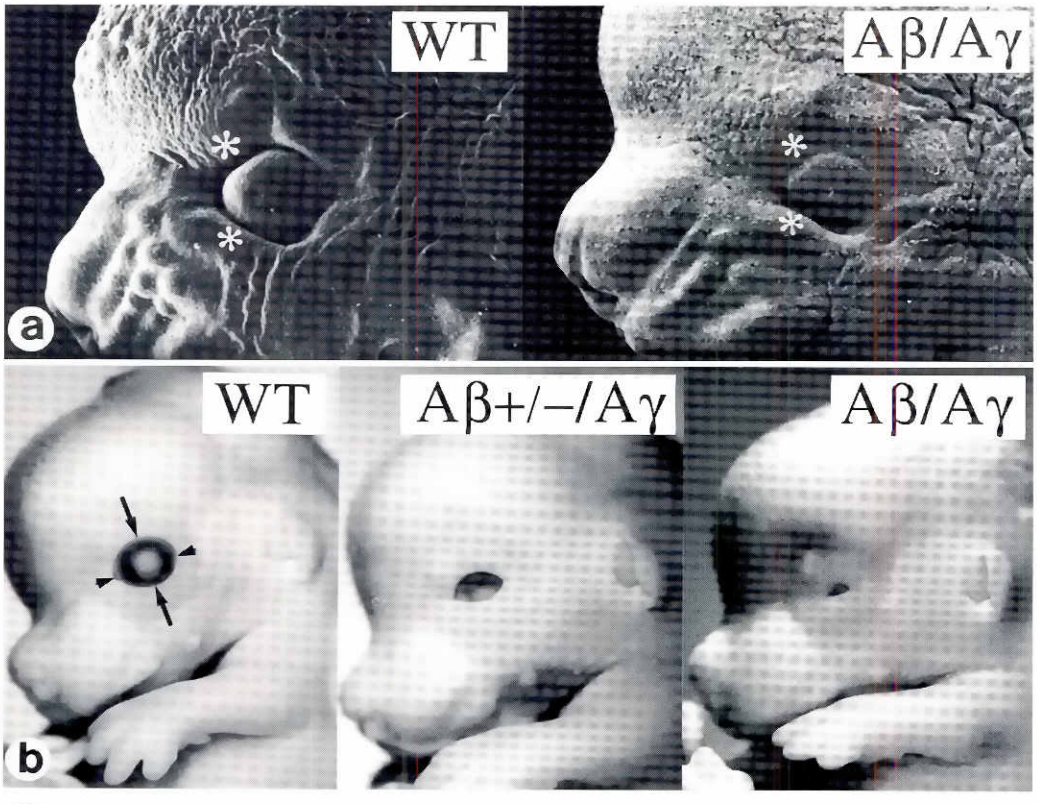

Fig. 4. Reduction of the palpebral aperture in RAR single and compound mutants (genotypes as indicated). (a) *Scanning electron micrograph of the eye region at E12.5; asterisks indicate the anlagen of the eyelids.* **(b)** *The eye region at E14.5: note that in all Aβ/Aγ mutants the palpebral aperture is reduced to a narrow slit. The spacing between the two arrowheads and the two arrows correspond to the intercanthal distance and height of the palpebral aperture respectively, whose measurements permitted to calculate the surface of the palpebral aperture as represented in* **(c). (d)** *Mean surfaces of the palpebral aperture are presented with standard errors (SEM). After testing for normality and variance homogeneity, results obtained for unpaired values were subjected to Student's t test between group of mice for each genotype. The 0.05 level was selected as the point of minimal statistic significance. Asterisks indicate the level of significance for the observed differences between +/+ and -/- mice (NS, not significant; **p<0.01 and ***p<0.001).*

the mutant RARβ RNA, as evidenced by the presence of a 179 nt long protected fragment (RARβ HR, Fig. 1e, left panel). In the RARβ$^{-/-}$ homozygotes, only the mutant form of RARβ RNA was present. Note that the level of expression of the mutant RNA was much lower than that of the WT form, presumably due to a decreased stability of the truncated mRNA. We cannot exclude that some RARβ peptides could be translated from the mutant mRNA. Nevertheless, these peptides would be terminated prematurely and lack both the LBD and the F region. Using a RARα probe, similar levels of the RARα2 and RARα1 transcripts were detected in WT, heterozygote or homozygote E13.5 embryos (Fig. 1e, middle panel). Additionally, there was no detectable change in the levels of RNAs encoding the RARγ1 and γ2 isoforms in the embryos lacking RARβ (Fig. 1e, right panel). These results indicate that RARβ does not play a unique role in controlling RARα and RARγ expression, and that no global compensatory increase of any of these isoforms occurred.

It is unlikely that the abnormalities observed in the present RARβ 'total' mutants could result from a dominant effect of the putative truncated peptides which could be translated from the lower level of mutant mRNAs for at least two reasons. Firstly, it was demonstrated that RARβ truncated at the level of the LBD does not exhibit any dominant negative effect on either DNA binding or transactivation by RARβ (Shen *et al.*, 1993; N.G. and P.C., data not shown). Secondly, heterozygous animals never displayed any defects. Thus, the present disruption of the RARβ gene most probably corresponds to a null mutation.

TABLE 2

MACROSCOPIC OCULAR ABNORMALITIES IN ADULT RARβ2 AND RARβ MUTANTS

	RAR mutant genotypes			
	Aβ2	Aβ+/-	Aβ	WT
Number of animals analyzed	8	16	36	14
Retrolenticular membrane or Persistent Hyperplastic Primary Vitreous (PHPV)	U:1/8 B:5/8	B:1/16	U:2/36 B:30/36	U:1/14
Cataract	0	0	B:3/36	0
Persistence of Bergmeister's papilla	ND	U:3/16 B:5/16	ND	U:7/14 B:3/14
Percentage of eyes with a PHPV	68%	6%	86%	3%

Adult mice were 3 to 8 months old. WT, wildtype; U, unilateral; B, bilateral; ND, not determined.

RARβ$^{-/-}$ (Aβ) mutants are growth deficient

To simplify the nomenclature, RAR isotype mutants for both alleles will be designated hereafter as Aα, Aβ and Aγ and the "$^{-/-}$" indicating homozygocity will be omitted. For example, RARβ$^{-/-}$, RARα$^{-/-}$/RARβ$^{-/-}$ and RARα$^{-/-}$/RARβ$^{+/-}$ mutants will be referred to as Aβ, Aα/Aβ and Aα/Aβ$^{+/-}$ mutants, respectively.

Aβ homozygotes were generated at the expected Mendelian frequency from intercrosses of Aβ+/- heterozygotes (Table 1), indicating that the RARβ mutation is not lethal during embryogenesis or post-natal development. Both Aβ males and females were fertile (Table 1) and lived as long as their WT littermates (at least 2 years). The weight of Aβ mutants was normal at birth but a weight decrease of ~20% in the female and of ~25% in the males was measured for the whole body, the liver and one of the leg muscles at post-natal day 20 (P20; Fig. 2 and data not shown). Similarly, a reduction (~10%) in the length of the tibia, fibula, femur and humerus was evidenced in Aβ mice as compared to WT (not shown). This harmonious post-natal growth retardation syndrome might reflect a decrease of growth hormone production (Bedo *et al.*, 1989).

RARβ$^{-/-}$ (Aβ) mutants display congenital defects in the ocular region and in the axial skeleton

Ocular defects

Examination of sections from adult (3 to 8 months old) Aβ eyes revealed in ~85% of the cases the presence within the vitreous body of an abnormal retrolenticular mass of pigmented tissue (R, Fig. 3c and d; compare with a and b) which exhibited a large base adherent to the lens (L) and contained a persistent hyaloid artery and vein (data not shown; see also H, Fig. 3g). This structure was

TABLE 3

ABNORMALITIES OF THE EYE AND ITS ADNEXAE IN RAR MUTANT FETUSES

	RAR mutant genotypes										
	Aα/Aβ		Aβ/Aγ		Aβ+/-/Aγ+/-	Aβ+/-/Aγ	Aβ/Aγ+/-	Aα/Aβ+/-	Aβ	Aγ	
Age of the fetuses	14.5	18.5	14.5	18.5	18.5	18.5	18.5	18.5	18.5	18.5	
Number of fetuses examined	3	6	5	7	6	8	6	5	5	10	VAD
Small conjunctival sac	0	0	B:#	B:#	ND	ND	ND	ND	0	0	+
Lens abnormalities											
Corneal-lenticular stalk	0	0	B:1/5	B:1/7	0	0	0	0	0	0	NR
Lens degeneration	0	0	0	B:#	0	0	0	0	0	0	+
Mesenchymal defects											
Agenesis of the corneal stroma	0	0	B:#	B:#	0	0	0	0	0	0	+
Agenesis of the iris stroma	NA (1)	0	NA (1)	B:#	0	0	0	0	0	0	+
Agenesis of the anterior chamber	NA (1)	0	NA (1)	B:#	0	0	0	0	0	0	+
Agenesis of the sclera	NA (1)	0	NA (1)	B:#	0	0	0	0	0	0	NR
Retrolenticular membrane (PHPV)	B:#	B:#	B:#	B:# Ch:#	B:5/6 (*)	B:# Ch:1/8	B:5/6	U:1/5 (*)	B:5/5	U:1/5 (*)	+
Retinal defects											
Shortening of ventral retina	0	0	B:#	NA (2)	ND	ND	ND	ND	0	0	+
Eversion of neural retina	0	0	U:2/5	U:2/7	ND	ND	ND	ND	0	0	+
Retinal dysplasia	0	0	B:3/5	B: #	ND	ND	ND	ND	0	0	+
Coloboma of the optic disk	0	0	B:2/5	U:3/7 B:2/7	ND	ND	ND	ND	0	0	+
Coloboma of the iris	0	0	U:1/5	0	ND	ND	ND	ND	0	0	+
Agenesis of Harderian glands	NA (1)	0	NA (1)	B:#	0	U:1/8 B:6/8	U:1/6	0	0	U:1/10 B:2/10	NR
Agenesis of naso-lacrimal duct	NA (1)	0	NA (1)	B:#	ND	ND	ND	ND	0	0	NR

#: these abnormalities are completely penetrant. U, unilateral; B, bilateral; NA, not applicable; (1) the corresponding structure is not yet formed at E14.5; (2) the relative lengths of the ventral and dorsal portions of the retina cannot be estimated at this stage due to extensive foldings; (*) very small retrolenticular membrane compared to that found in the other genotypes. ND, not determined; NR, not reported; Ch, chondrified; VAD, vitamin-A deficiency syndrome. for further details see text and Lohnes *et al.*, 1994.

bilateral in the vast majority (~94%) of the affected homozygotes and was only exceptionally observed in their heterozygote and WT littermates (Table 2).

A persistent and hyperplastic primary vitreous body (PHPV) represents the cause of the retrolenticular membrane (Traboulsi, 1993). The primary vitreous body is a transient embryonic structure consisting of fibroblastic cells stemming from the periocular mesenchyme and a capillary network given off by the hyaloid artery. By E13.5, the fibroblasts of the primary vitreous body (R, Fig. 3e) become dispersed within the rapidly expending secondary vitreous (SV, Fig. 3e), and are no longer identified at E15.5, except at the optic disk, forming the Bergmeister's papilla (or at least part of this structure; reviewed in Barishak, 1992 and Traboulsi, 1993). About 70% of our WT adult mice displayed a persistent Bergmeister's papilla (Table 2) taking the appearance of a conic mass of pigmented cells covering the optic disk (B, Fig. 3b).

Late E13.5 Aβ null and WT eyes were histologically indistinguishable (not shown). In particular, the closure of the optic fissure which suppresses the possibility of periocular cell migration into the optic cup, was achieved by this stage in both WT and Aβ mutants. However, in E14.5 Aβ fetuses the number of cell nuclei in the secondary vitreous was 4 to 6 times that of the WT (compare R, Fig. 3e and f and data not shown) and five E18.5 Aβ mutants showed a well defined, bilateral mass of densely packed cells behind the lens (Table 3, and data not shown). The first pigmented retrolenticular cells (see R in Fig. 3g) appeared at P4 concomitantly with the onset of appearance of melanin granules in the choroidal fibroblasts of both WT and Aβ mutants. These observations indicate that the loss of RARβ results in the maintenance and overproliferation of the fibroblastic neural crest cell (NCC)-derived component of the primary vitreous body (Johnston *et al.*, 1979).

Additional eye defects observed in Aβ null mice included congenital folds of the retina and cataracts, both of which are likely to be secondary to mechanical and/or metabolic stresses resulting from the presence of the PHPV. A single large fold of the neural retina was detected in 4 (out of 10) Aβ null eyes at E18.5 and was always confined to an area in contact with the retrolenticular membrane (F in Fig. 3g and data not shown). Cataracts were observed in ~8% of the adult Aβ mutants (Table 2) and characterized by a disruption of the lens basement membrane and disorganization of the lens fibers in contact with the PHPV (asterisk in Fig. 3d and data not shown).

Eyelids first appear at E12.5 (asterisks in Fig. 4a) and unite between E15 and E16.5 (Harris and McLeod, 1982). $A\beta^{+/-}$ and Aβ mutants analyzed at E14.5, i.e. before the onset of eyelid closure, displayed a mild reduction of the palpebral aperture compared to their WT littermates (Fig. 4c and d). A mild reduction of the palpebral aperture was also observed in E14.5 Aα, $A\gamma^{+/-}$ and Aγ fetuses (Fig. 4c and d). All 3 RARs are thus involved in the ontogenesis of the eyelids, probably through controlling the initial position of the origins of these structures (Fig. 4a and see below).

Axial skeletal defects

Homozygous RARβ mutants displayed some homeotic transformations and malformations of cervical vertebrae which were not previously observed in both RARβ2 (Mendelsohn *et al.*, 1994c) and RARβ mutants (Luo *et al.*, 1995). Four per cent of the Aβ mutants displayed a ventral median tubercle at the caudal edge of the basioccipital (BO) bone (TU, Fig. 5f compare with d), eventually fused with the anterior arch of the atlas (open white arrow in Fig. 5g). These features are indicative of a posterior homeotic transformation of the basioccipital bone (discussed in Lohnes *et al.*, 1993). Eleven per cent of the Aβ mutants displayed a posteriorization of the seventh cervical vertebra (posterior transformation of C7 to T1 in Table 4) characterized by the connection of this vertebra with a supernumerary rib fused ventrally to the first thoracic rib (Table 4, and data not shown). This transformation was usually unilateral and the ectopic C7 rib never contacted the sternum. Additionally, 10% of the Aβ mutants displayed malformations of the neural arches of the first three cervical vertebrae which were only exceptionally observed in WT fetuses (Table 4).

RARβ$^{-/-}$ (Aβ) mice have normal limbs

The present immunohistochemical data demonstrate the presence of the RARβ protein in the interdigital soft tissue and its apparent exclusion from the condensing precartilaginous blastema where the RARα and RARγ proteins are present (Fig. 6a-c); in the fetal limb, the distribution of RARα protein is ubiquitous and those of RARβ and RARγ proteins are apparently non overlapping. The interdigital expression of RARβ transcripts has suggested that this receptor might be involved in digit separation (Dollé *et al.*, 1989). It has also been proposed that RARβ2 could serve to prevent limb bud mesenchymal cells from expressing their chondrogenic bias in cultures (Jiang *et al.*, 1995). None of the fifty adult Aβ mutants analyzed in the present study displayed interdigital webbing and none of the seventy five E18.5 Aβ skeletal preparation showed any limb defect, thus providing definitive evidence that the RARβ is dispensable for both interdigital cell death and normal chondrogenesis of the limbs.

The nervous system of RARβ$^{-/-}$ (Aβ) mice is morphologically normal

Between E12.5 and E18.5, RARβ transcripts are confined to specific regions of the central nervous system including the

Fig. 5. Cranial and cervico-occipital skeletal defects in E18.5 RAR null mutants (genotypes as indicated). (a-c) *Dorsal views.* **(d-g)** *Ventral views.* **(h-k)** *Lateral views of the skull and nasal cavities.* **(l and m)** *Frontal histological sections at comparable levels of the nasal cavities [materialized by the black lines in* **(j)** *and* **(k)***]. AH and AV, horizontal and vertical portions of the alisphenoid bone; AL, alicochlear commissure, partially masked by the horizontal portion of the pterygoid bone (P); AAA, anterior arch of the atlas; B, basisphenoid bone; BO, basioccipital bone; C1 and C2, first and second vertebrae (atlas and axis) respectively; CF, carotid foramen; D, dentary bone; DN, dorsal nasal concha; E, exoccipital bone; E1-E3, ethmoturbinates; F, optic (cranial nerve II) foramen; G, gonial; HF, hypoglossal nerve (cranial nerve XII) foramen; JF, jugular foramen for cranial nerves IX, X and the jugular vein; MP, metoptic pillar; MS, maxillary sinus; MX, maxillary nerve; N, nasal septum; O, otic capsule; OB, orbitosphenoid bone; OF, oval foramen for the mandibular branch of cranial nerve V; OP, occipital process of the squamosal bone; P, pterygoid bone; PA, parietal bone; PP, prooptic pillar; PR, presphenoid bone; S, squamosal bone; ST, stapes; T, tympanic bone; TU, median tubercle of the basioccipital bone; V, vomer; VN, ventral nasal concha; VO, vomeronasal cartilage; Z, zygomatic (or jugal) bone; ZM, zygomatic process of the maxillar bone; ZS, zygomatic process of the squamosal bone. The small arrows in* **(a-c)** *indicate the limits of the 3 components of the zygomatic arch; the black open arrows in* **(b)***, the large black arrows in* **(c)** *and the white open arrow in* **(g)** *indicate the absent MP, the absent ZS and the BO-AAA-fusion, respectively. The double arrow in* **(e)** *indicates a fusion of the gonial and pterygoid bones. Same magnifications: in a-g, h and i; j,k: x12; l,m: x38.*

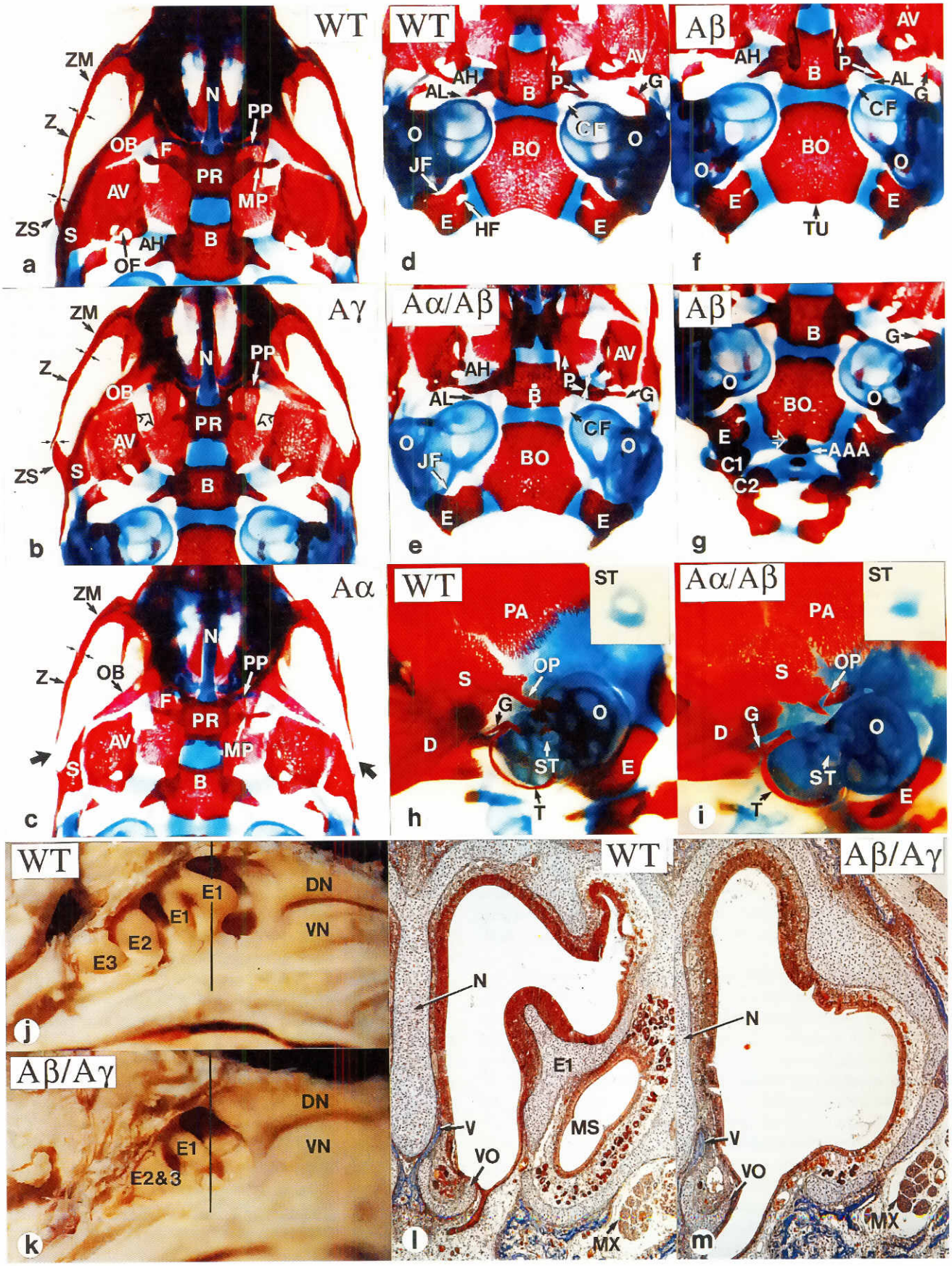
WT
ZM
Z
N
PP
OB
F
PR
AV
MP
ZS
S
AH
B
OF
a
WT
AV
AH
AL
P
G
O
BO
CF
JF
E
HF
d
Aβ
AV
AH
B
P
AL
G
CF
O
BO
E
TU
f
Aγ
b
Aα/Aβ
e
Aβ
C1
C2
AAA
g
Aα
c
WT
ST
PA
OP
S
G
D
T
h
Aα/Aβ
i
WT
Aβ/Aγ
E1
E2
E3
DN
VN
j
E2&3
k
V
VO
MS
MX
l
m

TABLE 4

AXIAL SKELETAL AND CARTILAGE ABNORMALITIES IN RAR MUTANTS

	RAR mutant genotypes									
	Aα	Aβ	Aγ	Aα/Aβ+/-	Aα+/-/Aβ	Aα/Aβ	Aβ+/-/Aγ	Aβ/Aγ+/-	Aβ/Aγ	WT
Total number of skeletons examined	15	75	12	15	15	8	14	13	13	80
Number of malformed skeletons	11 (73%)	27 (36%)	12 (100%)	15 (100%)	9 (60%)	8 (100%)	14 (100%)	6 (46%)	13 (100%)	13(16%)
Axial skeletal abnormalities										
Transformations										
Anteriorizations										
Anterior transformation of C2 to C1	1 (7%)	0	1 (8%)	3 (20%)	0	3 (38%)	2 (14%)	0	5 (38%)	0
Anterior transformation of C6 to C5						U:5 (63%)				
	0	0	0	0	0	B:1 (13%)	0	0	0	0
Anterior transformation of T8 to T7	3 (20%)	1 (1%)	5 (42%)	0	0	0	5 (36%)	0	4 (31%)	0
Anterior transformation of L1 to T14	U:1 (7%)			U:1 (7%)		U:3 (38%)				
	B:1 (7%)	0	0	B:5 (33%)	0	B:2 (25%)	0	0	0	0
Posteriorizations										
Posterior tubercle on Bo	0	2 (3%)	2 (17%)	0	0	0	2 (14%)	1 (8%)	5 (38%)	0
Fusion of Bo with C1-AA	0	1 (1%)	1 (8%)	0	0	1 (13%)	2 (14%)	0	3 (23%)	0
Posterior transformation of C7 to T1	3 (20%)	8 (11%)	0	0	1 (7%)	0	0	0	0	1 (1%)
Malformations										
Bo without hypoglossal nerve foramen	0	0	0	0	0	8 (100%)	0	0	0	0
Fusion of C1-AA with C2 dens	6 (40%)	15 (20%)	3 (25%)	8 (53%)	8 (53%)	5 (63%)	2 (14%)	3 (23%)	5 (38%)	11(14%)
C1 bifid	0	2 (3%)	1 (8%)	3 (20%)	0	1 (13%)	9 (64%)	0	NA	0
Dyssymphysis of C1 neural arch	0	2 (3%)	0	0	0	7 (88%)	0	0	13 (100%)	0
C2 bifid	0	5 (7%)	5 (42%)	5 (33%)	2 (13%)	2 (25%)	12 (86%)	2 (15%)	13 (100%)	1 (1%)
Fusions of neural arches of C2 and C3	1 (7%)	2 (3%)	1 (8%)	2 (13%)	0	4 (50%)	1 (7%)	0	6 (46%)	0
Sternum malformations	0	0	0	0	1 (7%)	0	0	1 (8%)	1 (8%)	0
Xiphoid process malformation	0	0	0	0	0	8 (100%)	0	0	0	0
Cartilage abnormalities										
Laryngeal cartilages										
Thyroid cartilage fused to hyoid bone	1 (7%)	0	0	1 (7%)	0	7 (88%)	0	0	0	0
Misshapen thyroid cartilage	0	0	0	0	0	8 (100%)	0	0	0	0
Misshapen arytenoid cartilage	0	0	0	0	0	8 (100%)	0	0	0	0
Misshapen cricoid cartilage	0	0	0	0	0	8 (100%)	0	0	0	0
Cricoid cartilage fused to tracheal rings	0	0	0	0	0	0	11 (79%)	0	13 (100%)	0
Tracheal cartilages	1 (7%)	0	11 (92%)	3 (20%)	0	8 (100%)	14 (100%)	0	13 (100%)	0

C1 to C7, first to seventh cervical vertebrae; T7 to T14, seventh to fourteenth thoracic vertebrae; L1, first lumbar vertebra; Bo, basioccipital; C1-AA, anterior arch of C1; U, unilateral; B, bilateral; NA, not applicable.

striatum (caudate-putamen and accumbens nucleus), the olfactory tubercle and the ventral column of the spinal cord (Ruberte *et al.*, 1993). At E18.5, all these structures strongly reacted with the anti-RARβ antibody, but not with the anti-RARα and anti-RARγ antibodies (A, CP and OT in Fig. 6d-e, and data not shown). The same pattern of RARβ protein distribution was maintained in the adult brain and spinal cord (CP in Fig. 6f, and data not shown). However, histological analysis of E18.5 and adult Aβ mutant brains, which as expected were devoid of RARβ immunostaining (Fig. 6g, and data not shown), did not reveal any abnormality (e.g. Fig. 7d and e).

A bilateral fusion of the proximal portions of the glossopharyngeal and vagus nerves (cranial nerves IX and X respectively) represents the only malformation reported by Luo *et al.* (1995) in Aβ mutants. These authors therefore suggested that the loss of RARβ function might lead to localized disruption of the patterning of the hindbrain region corresponding to rhombomeres 6 and 7. To determine the actual penetrance of this nerve fusion, we performed whole-mount anti-neurofilament immunostaining on 91 Aβ homozygotes, 106 heterozygotes and 40 WT littermates at E10.5 (Fig. 7a-c). Five (5.5%) Aβ, 4 (4.7%) $A\beta^{+/-}$ and 2 (5%) WT animals displayed a unilateral fusion (open arrow) of the proximal portion of the glossopharyngeal (N9) and vagus (N10) nerves. Therefore, in the genetic background of our mice, this nerve fusion occurs independently from the RARβ mutation.

Analysis of $RAR\alpha^{-/-}/RAR\beta^{-/-}$ (Aα/Aβ) and $RAR\beta^{-/-}/RAR\gamma^{-/-}$ (Aβ/Aγ) compound mutants

Compound RARα/RARβ and RARβ/RARγ null mutants were produced from intercrosses of $RAR\beta^{+/-}/RAR\alpha^{+/-}$ or $RAR\beta^{+/-}/RAR\gamma^{+/-}$ double heterozygotic mice, respectively. The Mendelian distribution of $A\alpha^{+/-}/A\beta$, $A\alpha/A\beta^{+/-}$, Aα/Aβ, $A\beta^{+/-}/A\gamma$, $A\beta/A\gamma^{+/-}$ and Aβ/Aγ double mutant offspring at E18.5 indicated that the loss of these receptors did not result in embryonic lethality (not shown). However, in contrast to all other single null mutants or compound mutants, the Aα/Aβ and Aβ/Aγ mutants invariably died within at most 12 h following cesarian delivery at E18.5.

Soft tissue defects in $RAR\alpha^{-/-}/RAR\beta^{-/-}$ (Aα/Aβ) mutants

Each Aα/Aβ fetus displayed multiple visceral abnormalities (Tables 5, 6 and 7), most of which are incompatible with life after birth, affecting the respiratory tract (e.g. lung agenesis or hypoplasia, agenesis of the oesophagotracheal septum), the heart outflow tract (e.g. persistent truncus arteriosus, high ventricular septal defect), the arteries destined to the head and forelimbs (summarized in Table 7), the digestive tract (i.e. agenesis of the anal canal), the kidneys and ureters (kidney hypoplasia; hydronephrosis probably secondary to ectopic ureteral openings or involution of the caudal ureter), and the female genital tract (i.e. agenesis of the oviduct, uterus and cranial vagina). The majority of these abnormalities belong to the fetal VAD syndrome (see VAD in Tables 5 and 6).

With the exception of the retrolenticular membrane, the Aα/Aβ abnormalities were never observed in either Aα or Aβ single mutants. However, most of them have been previously found in Aα/Aβ2 mutants (Mendelsohn *et al.*, 1994b), with the notable exceptions of agenesis of the stapedial artery, thymus agenesis or severe ectopias, absence of the spleen and defects of the inferior vena cava.

Agenesis of the stapedial artery

This artery represents an important morphological landmark, since it corresponds to the remnant of the 2nd aortic arch; its passage through the precartilaginous blastema of the stapes determines the horseshoe shape of this middle ear ossicle (Diamond, 1989, and references therein). Unilateral and bilateral agenesis of the stapedial artery was observed on serial histological sections of some Aα/Aβ fetuses and was invariably associated with the absence of the intercrural foramen of the stapes (Table 5 and data not shown). Furthermore, this bony defect was bilaterally observed in some Aα/Aβ skeletons (ST, compare Fig. 5 h and i; Table 8). It is noteworthy that these arterial and skeletal defects were not specific of one particular combination of disrupted RARs as they were also detected with lower frequencies in Aα1/Aγ, Aα/Aβ2, Aβ2/Aγ, and Aβ/Aγ mutants (Tables 5 and 8, V.D. and M.M. unpublished results). That the stapedial artery is lacking in some RAR compound mutants extends our previous observations indicating that these nuclear receptors play an important role in the ontogenesis of NCC-derived arterial smooth muscle cells (Mendelsohn *et al.*, 1994b).

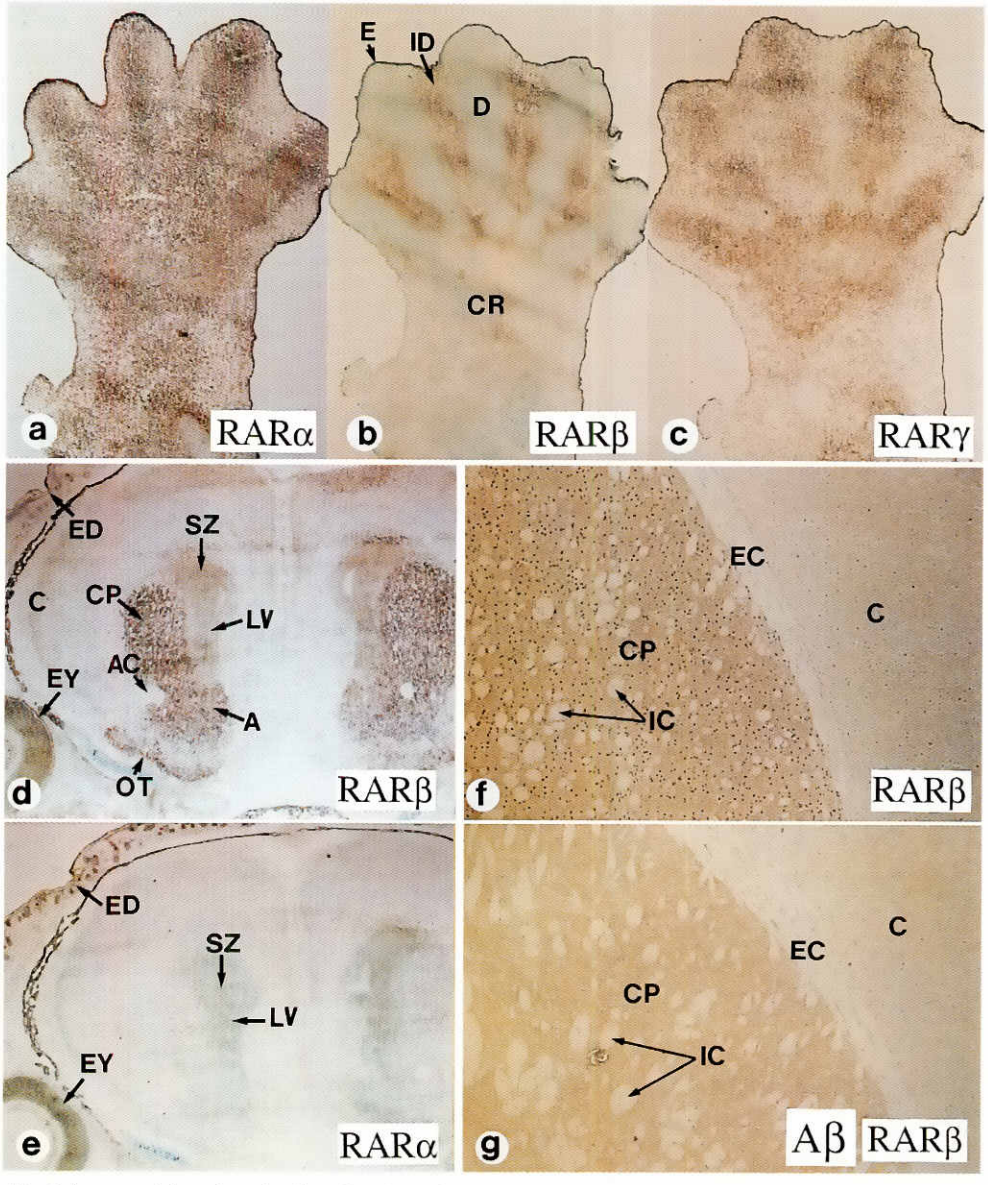

Fig. 6. Immunohistochemical localization of RARα, RARβ and RARγ (as indicated) in E13.5 limbs (a-c) and newborn (d and e) and adult (f and g) brain. *All the tissues are from WT mice except* **(g)** *where the anti-RARβ antibody was applied on a brain section from an Aβ mutant. A, accumbens nucleus; AC, anterior commisure; C, cerebral cortex; CP, caudate-putamen; CR, precartilaginous anlagen of the carpal bones; D, digit; E, ectoderm; EC, external capsule; ED, epidermis; EY, eye; IC, internal capsule; ID, interdigital mesenchyme; LV, lateral ventricle; OT, olfactory tubercle; SZ, subventricular zone. Magnifications: a-c: x26; d,e: x16; f and g: x41.*

Thymic agenesis and ectopia and absence of the spleen

The Aα/Aβ thymic phenotype represents the only obvious example of developmental defects whose severity is increased as compared to the Aα/Aβ2 situation (Table 5). A complete thymic lobe in the neck region (i.e. a persistent cervical thymus) and /or the absence of one or both thymic lobes were consistently observed in Aα/Aβ mutants, but not in Aα/Aβ2 mutants, which however displayed milder forms of thymic ectopias (i.e. accessory cervical thymus bodies and aberrant pharyngeal lymphoid tissue; Mendelsohn *et al.*, 1994b). Thymic agenesis and ectopias generated in chicken by ablation of post-otic rhombencephalic NCC are always associated with defects of the heart outflow tract or aortic arches and sometimes with thyroid agenesis or hypoplasia (Bockman and Kirby, 1984). That this spectrum of malformations is completely recapitulated in some Aα/Aβ (as well as in some Aα/Aγ mutants; Mendelsohn *et al.*, 1994b) is consistent with our previous hypothesis of a mesectodermal deficiency in mice lacking RARs (Mendelsohn *et al.*, 1994b; Kastner *et al.*, 1995).

Spleen agenesis was observed in only one (out of 9) Aα/Aβ mutants (Table 5). However, since this abnormality was absent in the dozens of WT and mutant fetuses that we have analyzed (including Aα/Aγ), it might reflect a specific developmental function of RARβ1/β3 isoforms in spleen.

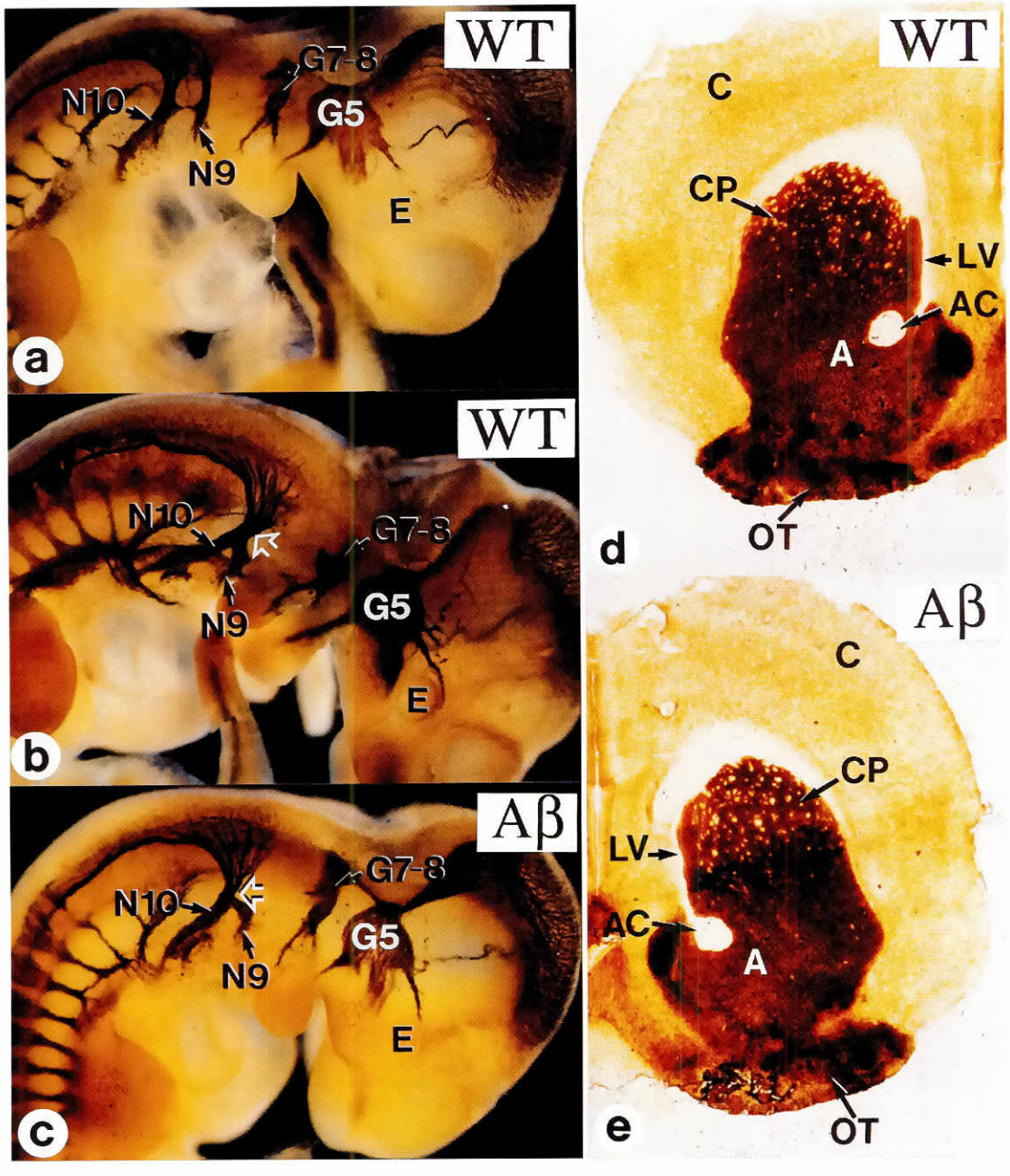

Fig. 7. Comparison of the cranial nerves and brain of WT and Aβ mutants. (a-c) *E10.5 embryos immunolabeled with a monoclonal antibody (2H3) against a neurofilament protein.* **(d and e)** *Frozen sections from adult brain stained for the demonstration of acetylcholinesterase activity (Paxinos and Watson, 1986). A, accumbens nucleus; AC, anterior commissure; C, cerebral cortex; CP, caudate putamen; E, eye; G5 and G7-8, ganglion of cranial nerve V and facial-acoustic ganglia, respectively; LV, Lateral ventricle; N9 and N10, cranial nerves IX and X; OT, olfactory tubercle; the open arrow indicates the fusion between these two nerves. Magnification: d-e: x15.*

Defects of the inferior vena cava

Abnormal development of the embryonic venous system can result in absence of the hepatic and prerenal portions of the inferior vena cava (absence of the inferior vena cava; Table 5), or in the presence of both right (i.e. normal) and left (i.e. supernumerary) inferior vena cava below the renal veins (double inferior vena cava; Table 5). These two abnormalities were observed with the same low penetrance in Aα/Aβ mice (present data) and Aα/Aβ2 mice (our unpublished results). It is noteworthy that in Aα/Aβ (Aα/Aβ2) mice as in human patients, absence of the inferior vena cava was always associated with, and thus might be secondary to a variety of congenital heart defects (Gray and Skandalakis, 1972).

Soft tissue defects of RARβ$^{-/-}$/RARγ$^{-/-}$ (Aβ/Aγ) mutants

As expected from our previous analysis of Aβ2/Aγ mutants (Lohnes *et al.*, 1994; Mendelsohn *et al.*, 1994b), Aβ/Aγ mutants displayed severe ocular defects (Table 3), and a high frequency of hydronephrosis most likely caused by abnormalities of the caudal ureters (Table 6). Abnormalities of the great arteries derived from the 3rd, 4th and 6th aortic arches which were absent in the 3 previously analyzed Aβ2/Aγ were here observed in ~25% of the Aβ/Aγ mutants (Tables 5 and 7). Some of the ocular malformations which we previously overlooked in Aβ2/Aγ mutants, including defects in mesenchymal structures (sclera, iris and secondary vitreous), congenital cataracts, shortening of the ventral retina and pre-natal retinal dysplasia will be described here.

TABLE 5

ABNORMALITIES OF THE RESPIRATORY SYSTEM, HEART OUTFLOW TRACT, BLOOD VESSELS AND GLANDS IN RAR DOUBLE MUTANTS

	RAR mutant genotypes				
	Aα/Aβ		Aβ/Aγ		
Age of the fetuses	14.5	18.5	14.5	18.5	
Number of fetuses examined	3	6	5	7	VAD
Respiratory system abnormalities					
Agenesis of left lung	#	5/6	0	0	+
Hypoplastic left lung	0	1/6	0	0	+
Hypoplastic right lung	#	#	0	0	+
Lack of œsophagotracheal septum	#	#	0	0	+
Diaphragmatic hernia	0	3/6	0	0	+
Heart outflow tract and vascular defects					
Persistent truncus-arteriosus (NCC)	#	#	0	0	+
Absence of cono-truncal septum (E14.5)/high VSD (E18.5)	#	#	0	0	+
Abnormal arteries derived from Ao.A. 3-6 (NCC)	#	#	1/5	2/7	+
Agenesis of the stapedial artery (NCC)	B:1/3	U:2/6	0	U:1/7	NR
Double inferior vena cava	ND	2/6	0	0	NR
Absence of the inferior vena cava	ND	1/6	0	0	NR
Glandular abnormalities					
Persistent cervical thymus (NCC)	U:3/3	U:4/6 B:1/6	0	0	NR
Thymus agenesis (NCC)	U:2/3	U:1/6 B:1/6	0	0	NR
Thyroid hypoplasia (NCC)	ND	U:1/6	0	0	NR
Shortening of the sublingual duct	NA	U:1/6 B:1/6	NA	B:#	NR
Shortening of the submandibular duct	NA	0	NA	0	NR
Spleen agenesis	0	1/6	0	0	NR

#: these abnormalities are completely penetrant. U, unilateral; B, bilateral; NA, not applicable: these ducts are not fully formed at E14.5; NR, not reported; ND, not determined; VAD, vitamin-A deficiency syndrome; high VSD, high ventricular septal defect: this abnormality represents the manifestation at E18.5 of the lack of formation of the cono-truncal septum observed in E14.5 mutants; Ao.A. 3-6: third, fourth and sixth aortic arches; NCC, these defects are likely caused by abnormal migration, proliferation, death or differentiation of neural crest cells. See Mendelsohn *et al.*, 1994b for further details, and Table 3 for additional glandular abnormalities in the eye region.

Defects of ocular structures derived from the mesectoderm

In Aβ/Aγ mutants, the corneal stroma (CS, Fig. 8e and i), that of the iris (IS, Fig. 8i) and the anterior chamber of the eye (A, Fig. 8e and i) were consistently absent and replaced by a thick layer of loosely organized mesenchyme filling the space between the lens and the (small) conjunctival sac or the surface ectoderm (M, Fig. 8b,f and j); the sclera was never identified (S in Fig. 8e and g compare with f and h); the primary vitreous body filled completely the space between the retina and the lens due to extensive cell proliferation (demonstrated by the presence of numerous mitotic figures; data not shown) and to the lack of formation of the secondary vitreous (see R, Fig. 8b,f and h). Local aberrant differentiation of the ocular mesenchyme into cartilage was always observed within the vitreous body (CA, Fig. 8h).

Lens abnormalities

The histological structure of the Aβ/Aγ lenses was normal at E14.5 (compare L, Fig. 8a and b). In contrast, in all Aβ/Aγ lenses seen at E16.5 and E18.5, the equatorial cells were missing (L, Fig. 8f and j) and the secondary fibers displayed features of degeneration (i.e. swelling and vacuolation of their cytoplasm; L, Fig. 8j, and data not shown).

Retinal defects

Shortening of the ventral retina and pre-natal retinal dysplasia represent the only two abnormalities of the fetal VAD syndrome not previously detected in RAR compound mutants. In all E14.5 Aβ/Aγ mutants, the ventral portion of the retina was bilaterally reduced in size with respect to its dorsal counterpart (compare V and D, Fig. 8a,b). This defect was consistently associated with a ventral rotation of the lens (L, Fig. 8b), as it is also the case in RXRα null mutants where these two abnormalities were first described (Kastner *et al.*, 1994).

The normal E14.5 mouse neural retina shows two layers of nuclei, the outer and inner neuroblastic layers (ONL and INL respectively, Fig. 8c) which, at E16.5, become separated by a layer of cell processes, the primitive inner plexiform layer (IPL). Mitotic figures (arrow in Fig. 8c) are confined to the outermost ONL cells. In 3 out of 5 E14.5 Aβ/Aγ mutants, large extracellular pockets of empty space (vacuoles, VA in Fig. 8d) were observed between the neuroblasts located at the interface of the ONL and the INL. Cells with irregular outlines and excentrically-positioned nuclei, possibly corresponding to macrophages (large arrows Fig. 8d), were frequently observed within these vacuoles. As these macrophage-like cells often displayed mitotic figures (double arrows in Fig. 8d), the presence of ectopic cell division was a striking feature of the dysplastic phenotype at this developmental stage. In the eyes of the two Aβ/Aγ mutants analyzed at E16.5 and in all E18.5 Aβ/Aγ eyes, some vacuoles had apparently merged into larger cavities (CV, Fig. 8f). Moreover, at 18.5 dpc, the IPL was essentially lacking and the neural retina showed extensive foldings (compare Fig. 8g and h, and data not shown). Interestingly, a similar retinal dysplasia

TABLE 6

ABNORMALITIES OF THE UROGENITAL AND DIGESTIVE TRACTS IN RAR DOUBLE MUTANTS

	RAR mutant genotypes				
	Aα/Aβ		Aβ/Aγ		
Age of the fetuses	14.5	18.5	14.5	18.5	
Number of fetuses examined (males : females)	3	1:5	5	5:2	VAD
Kidney abnormalities					
Renal hypoplasia	B:#	B:#	0	0	+
Hydronephrosis		U:2/6		U:2/7	
	0	B:3/6	0	B:1/7	+
Ureter abnormalities					
Agenesis of caudal ureter				U:2/7	
	0	U:1/6	0	B:1/7	+
Ectopic ureteral openings (a)		U:2/6	U:1/5	U:1/7	
	B:#	B:4/6	B:2/5	.	+
Agenesis of the Müllerian duct (E14.5 fetuses) or of its derivatives (E18.5 females) (b)					
Complete	B:#	B:#	0	0	+
Partial (caudal portion missing)			U:1/5		
	NA	NA	B:2/5	0	+
Agenesis of the anal canal	#	#	0	1/7	NR

#: these abnormalities are completely penetrant. U, unilateral; B, bilateral; NA, not applicable; NR, not reported; VAD, vitamin-A deficiency syndrome. (a): opening of the ureter in the terminal portion of the Wolffian duct and/or common openings of the Wolffian duct and ureters in the uro-genital sinus (E14.5) or opening of the ureters in the urethra (E18.5); (b): absence of the oviducts, uterus and cranial vagina.

TABLE 7

DEFECTS OF ARTERIES IN RAR DOUBLE MUTANTS

	RAR mutant genotypes	
Number of fetuses examined	Aα/Aβ 9	Aβ/Aγ 12
Arch of the aorta on the right side	2/9	1/12
Arch of the aorta on the right side; retroœsophageal left subclavian artery	4/9	1/12
Arch of the aorta on the right side and located in the cervical region; retroœsophageal left subclavian artery	1/9	0
Retroœsophageal right subclavian artery	0	1/12
Aberrant origin of the right pulmonary artery from ipsilateral arch of the aorta	1/9	0
Aberrant origin of the right pulmonary artery from ipsilateral common carotid; retroœsophageal right subclavian artery	1/9	0

Defects of the arteries normally derived from aortic arches 3 (i.e., common carotid), 4 (i.e., arch of the aorta, subclavian arteries) and 6 (i.e., pulmonary arteries) in RAR double mutants. For further details see Mendelsohn *et al.*, 1994b.

is also observed in some RXRα null mutants at E14.5 (our unpublished results).

Ocular defects of RARβ$^{-/-}$ (Aβ) mutants are increased in RARα$^{-/-}$/RARβ$^{-/-}$ (Aα/Aβ) and in RARβ$^{-/-}$/RARγ$^{-/-}$ (Aβ/Aγ) compound mutants

The severity of the reduction of the palpebral aperture measured in E14.5 Aβ$^{+/-}$ and Aβ single mutants was increased in all compound mutants of RARβ and RARγ and also, albeit to a lesser extent, in all compound mutants of RARβ and RARα (Fig. 4b-d). In Aβ/Aγ mutants the palpebral aperture was reduced to small narrow slit (Fig. 4b). The dorsal and ventral folds representing the origins of the eyelids at E12.5 were much closer to one another in Aβ/Aγ mutants than in WT embryos (asterisk in Fig. 4a). In severely affected viable, double mutants (i.e. Aβ/Aγ$^{+/-}$ and Aβ$^{+/-}$/Aγ, Fig. 4b-d), the outcome of this abnormality was a blepharophimosis, i.e. a severe reduction of the definitive palpebral aperture which can be diagnosed after eyelid opening by P14 (not shown; see also Grondona *et al.*, 1996).

Unexpectedly, a high frequency of PHPV was observed following disruption of only one allele of the RARβ gene in a Aγ and Aγ$^{+/-}$ genetic background (Table 3). In the case of E18.5 Aβ$^{+/-}$/Aγ$^{+/-}$ mutants, this PHPV was small and was not directly connected with the main hyaloid vessels at the optic disk; it was never observed in the twenty Aβ$^{+/-}$/Aγ$^{+/-}$ adult eye. A possible explanation for this discrepancy is that the Aβ$^{+/-}$/Aγ$^{+/-}$ PHPV is not large enough to elicit the maintenance of its own vascular supply and thus disappears together with the hyaloid system by P14.

Skeletal defects of RARα$^{-/-}$/RARβ$^{-/-}$ (Aα/Aβ) and of RARβ$^{-/-}$/RARγ$^{-/-}$ (Aβ/Aγ) compound mutants

Homeotic transformations and other vertebral defects

Aα/Aβ and Aβ/Aγ compound mutant mice exhibited homeotic transformations absent from the Aβ single mutants (Table 4). Malformations of the axial skeleton were also observed (Table 4). In particular, all Aα/Aβ mutant fetuses lacked the foramen of the hypoglossal nerve (HF in Fig. 5d, compare with Fig. 5e). Amongst vertebral defects, dyssymphysis of the neural arch of C1 represented the only obvious example of defect whose severity was increased in Aα/Aβ and Aβ/Aγ mutant as compared to the Aα/Aβ2 and Aβ2/Aγ situation (Lohnes *et al.*, 1994). The xiphoid process of all the Aα/Aβ mutants (Table 4, and data not shown), on which two supernumerary ossified horns were observed, displayed a delayed ossification.

Cranial skeletal defects

With the exception of the pterygoquadrate element, craniofacial skeletal defects have only been reported in Aα/Aγ and Aα1/Aα2$^{+/-}$/Aγ compound mutants (Lohnes *et al.*, 1994). In the course of the present study, we incidentally discovered discrete cranial skeletal abnormalities in Aα and Aγ single mutants as well as in compound mutants of either RARβ and RARα or RARβ and RARγ (Table 8). A pterygoquadrate element, previously shown to occur in various compound mutants of RARα1 and of RARα (Lohnes *et al.*, 1994), was here observed in ~10% of the Aα mutants (Table 8). Agenesis or severe hypoplasia of the zygomatic process of the squamosal bone (ZS) was seen in about one third of the Aα mutants, resulting in a caudal gap of the zygomatic arch (compare Fig. 5a and c). A complete absence of the metoptic pillar (MP, Fig. 5a), the caudal limit of the optic nerve foramen (F, Fig. 5a) was observed in some Aγ null fetuses (open arrows in Fig. 5b).

The penetrance of these 3 skeletal defects increased in a graded manner upon the inactivation of one and of both alleles of the RARβ gene from either the Aα null genetic background (i.e. pterygoquadrate element, agenesis of the zygomatic process) or the Aγ null genetic background (i.e. agenesis of the metoptic pillar). Additionally, in Aα/Aβ$^{+/-}$ and Aα/Aβ mutants the extent of the squamosal malformation was markedly increased (e.g. compare the normal occipital process of the squamosal, OP, in Fig. 5h with the misshapen OP in Fig. 5i). Cranial skeletal abnormalities observed only in the double null mutants included: (i) hypoplasia of the caudal ethmoturbinates (E2 and E3 in Fig. 5j and k), partial agenesis of the rostral ethmoturbinate (E1, compare Fig. 5j and l with Fig. 5k and m) and absence of the maxillary sinus (MS compare Fig. 5l with m) in the nasal cavity of Aβ/Aγ mutants and (ii) abnormal shape of the gonial bone (G in Fig. 5d-i), which corresponds to the anlage of the malleus anterior process, in Aα/Aβ mutants.

All Aα/Aβ and Aβ/Aγ compound mutants also showed laryngeal cartilage malformations (Table 4) identical to those described in Aα/Aβ2 and Aβ2/Aγ mutants by Mendelsohn *et al.* (1994b).

Interdigital webbing in RARβ$^{-/-}$/RARγ$^{-/-}$ (Aβ/Aγ) mutants

In E13 WT embryos, the indentation of the handplate and footplate indicates the onset of digit separation (Wanek *et al.*, 1989) which is completed by E14 in the forelimb and by E15 in the hindlimb (e.g. Fig. 9e). Separation of the digits is followed by their reunion by epithelial fusion between E16 and E17 (Maconnachie, 1979), then digits stay fused for the first 4 days of post-natal life (Wanek *et al.*, 1989).

A striking feature of the E18.5 Aβ/Aγ skeleton was the claw shape of the fore- and hindlimb digits which were also divergent instead of being straight and nearly parallel to one another as in WT fetuses (Fig. 9a). Histological sections through these E18.5 mutant limbs showed an absence of the epithelial lamina normally con-

necting the digits (EL, Fig. 9b). To investigate the origin of these abnormalities, limbs of Aβ/Aγ fetuses were compared to those of weight-matched littermates on scanning electron micrographs (Fig. 9e). In E16.5 mutants, the interdigital epithelial ridges (white arrow, Fig. 9e) which are hallmarks of digital reunion were absent and at E15.5 the mutant digits were not separated. Moreover, at E14.5 and E16.5 the digits appeared broader than their WT counterparts. Taken together, these observations indicate that the skeletal abnormalities of the digits (Fig. 9a) and their absence of epithelial connection at birth (Fig. 9b) are likely to be caused by an absence of involution of the interdigital mesenchyme between E13.5 and E15.5. As already mentioned, Aβ/Aγ do not survive for more than a few hours after birth. However, the final outcome of the limb abnormalities could be seen in adult $Aβ^{+/-}$/Aγ mutants which consistently displayed interdigital webbing affecting all digits of both hand and foot (Fig. 9c and d). In contrast, this abnormality was not observed in E18.5 Aα/Aβ mutants nor in adult Aβ/$Aγ^{+/-}$ mutants, thus further indicating that RARγ is the main RAR involved in the involution of the interdigital mesenchyme.

Discussion

Functions of RARβ during embryonic development

A detailed morphological analysis allowed us to uncover abnormalities that we had previously overlooked in single and double mutants of RARα, RARβ2 and RARγ (Lohnes *et al.*, 1993, 1994; Lufkin *et al.*, 1993; Mendelsohn *et al.*, 1994b,c) and to rule out the proposal that the patterning of cranial nerves IX and X could be critically dependent on RARβ (Luo *et al.*, 1995). In addition, careful comparisons of the phenotypes of single or compound mutants of either RARβ2 (Mendelsohn *et al.*, 1994b,c; Grondona *et al.*, 1996) or RARβ did not reveal outstanding differences with the possible exceptions of spleen and thymus ageneses, which were found only in Aα/Aβ mutants. However, it is noteworthy that thymus agenesis occurred with similar frequency in compound mutant fetuses lacking the RXRα gene and either all RARβ isoforms (RARβ 'total') or the RARβ2 isoform only (Kastner *et al.*, 1997). In contrast, the heart of RXRα/RARβ double mutants always lacked the cono-truncal septum, a defect which was only rarely observed in RARβ2/RXRα double mutants (Kastner *et al.*, 1997). Whether this difference between the occurrence of the thymus and cono-truncal septum defects reflects a specific role of RARβ1/β3 or merely a gene dosage effect will await the generation of RARβ1/β3 mutant mice.

Eye development

RARβ is required for the normal involution of the fibroblastic component of the primary vitreous body. This function is largely fulfilled by the β2 isoform, as ~70% of the RARβ2 mutants also display a PHPV (Grondona *et al.*, 1996). Interestingly, PHPV represents the most common abnormality of the rat fetal VAD syndrome (Warkany and Schraffenberger, 1946). However, the rare occurrence of PHPV and high frequency of persistent Bergmeister's papilla (which might be assimilated to a partial PHPV) in our WT mice clearly indicate that RARβ is not the sole factor involved in the regression of the primary vitreous body. In this respect, we also note that PHPV has been observed in transgenic mice which overexpress TGFα in the eye globe (Renecker *et al.*, 1995) or in which ocular macrophages have been ablated by expression of the diphtheria toxin from a macrophage specific transgene (Lang and Bishop, 1993). The RARβ mutation may prevent cell death and/or elicit overproliferation of a subset of periocular mesenchymal cells. However, it has no apparent effect on cell differentiation, since the cells of the PHPV give rise to melanocytes, one of the two main overtly differentiated cell types (with scleral fibroblasts) found in the periocular envelopes. It has been shown that RARβ2 is transcriptionally upregulated in senescent human dermal fibroblasts and human mammary epithelial cells (Si *et al.*, 1996 and references therein). These latter data, combined with studies showing that certain tumor cell lines have

TABLE 8

ABNORMALITIES OF THE CRANIAL SKELETONS IN RAR MUTANTS

	RAR mutant genotypes												
	Aβ+/-	Aβ	Aγ+/-	Aγ	Aβ+/- Aγ+/-	Aβ+/- Aγ	Aβ Aγ	Aβ Aγ+/-	Aα	Aα Aβ+/-	Aα Aβ	Aα+/- Aβ	WT
Number of skeletons examined	50	50	7	15	12	14	13	14	15	14	6	15	26
Hypoplasia of ethmoturbinates	0	0	0	0	0	ND	#	ND	0	0	0	0	0
Agenesis of metoptic pillar	7/50	15/50	0	11/15	4/12	11/14	12/13	10/14	1/15	1/14	0	2/15	4/26
Partial	U:3/50 B 4/50	U:8/50 B:7/50	0	U:5/15 B:5/15	U:2/12 B:2/12	U:5/14 B:1/14 U:3/14	U:1/13	U:3/14 B:7/14	U: 1/15	U:1/14	0	U:2/15	U:2/26 B:2/26
Complete	0	0	0	U:2/15	0	B:4/14	B:11/13	0	0	0	0	0	0
Pterygoquadrate element	0	0	0	0	0	0	0	0	U:2/15	U:3/14 B:4/14	U:3/6 B:1/6	0	0
Abnormal gonial bone	0	0	0	0	0	0	0	0	0	0	U:1/6 B:2/6	0	0
Squamosal malformed	0	0	0	0	0	0	0	0	B:4/15	B:11/14	B:#	0	0
Imperforated stapes	0	0	0	0	0	0	U:1/13	0	0	0	B:2/6	0	0

Note that the abnormalities of the occipital bone have been listed in Table 4 since this bone represents, in ontogenic terms, a modified vertebra. #, this abnormalities is completely penetrant; U, unilateral; B, bilateral; ND, not determined.

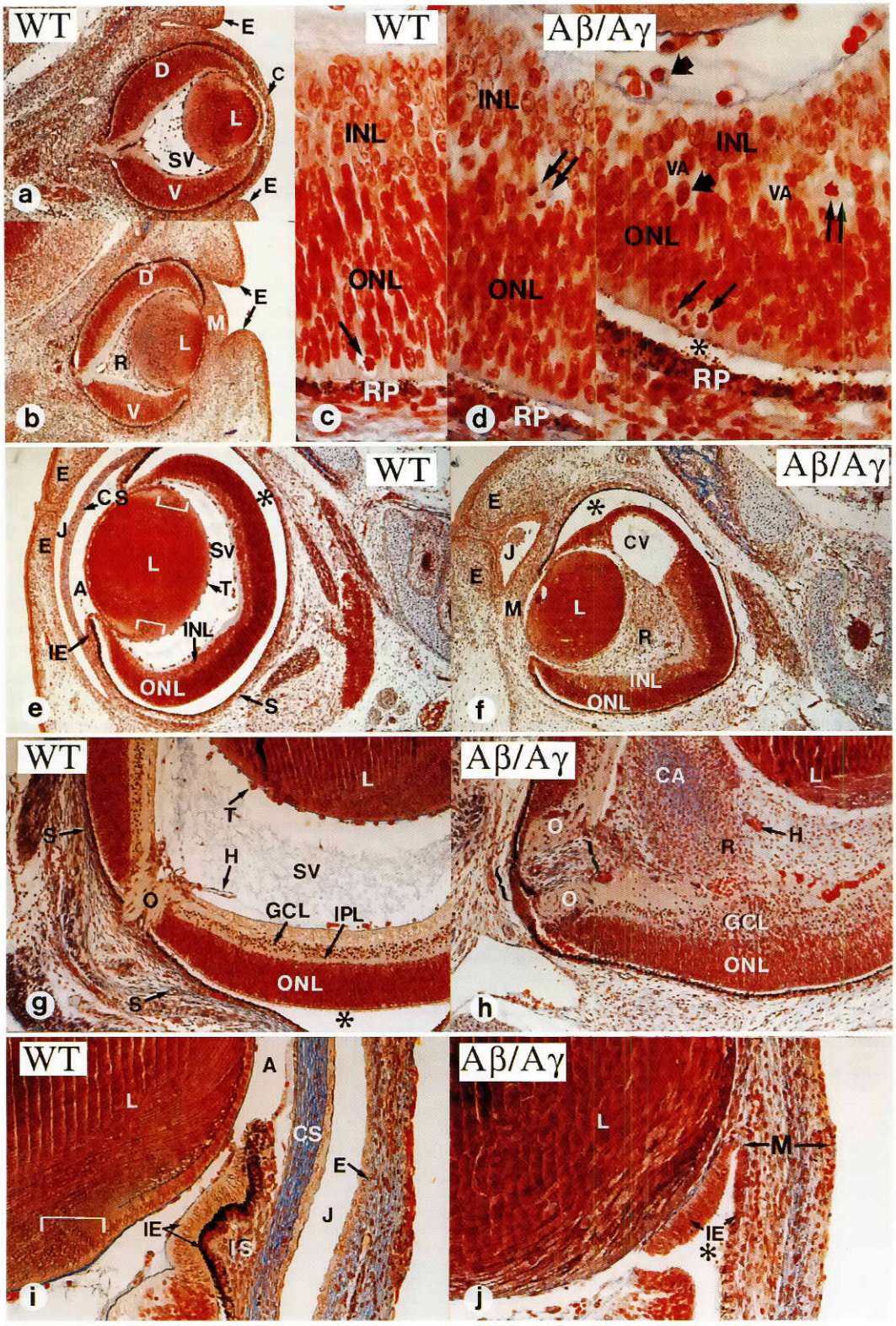

Fig. 8. Eye defects in double null mutants of RARβ and RARγ. *Frontal histological sections from E14.5* **(a-d)**, *E16.5* **(e,f)** *and E18.5* **(g, j)** *WT* **(a,c,e,g and i)** *and Aβ/Aγ mutants* **(b,d,f,h and j)**. *A, anterior chamber; C, cornea; CA, cartilage; CS, corneal stroma; CV, an example of cavity in the neural retina; D, dorsal retina; E, eyelids; GCL, ganglion cell layer; H, hyaloid vessels; IE, epithelial portion of the iris; IS, stroma of the iris; INL, inner neuroblastic layer; IPL, anlage of the inner plexiform layer; J, conjunctival sac; L, lens; M, undifferentiated mesenchyme; O, optic nerve; ONL, outer neuroblastic layer; R, retrolenticular membrane; RP, retinal pigment epithelium; S, sclera; SV, secondary vitreous; T, vascular capsule of the lens (tunica vasculosa lentis); V, ventral retina; VA, vacuoles. The thin arrows, double arrows and thick arrows in (c) and (d) point to normal mitotic figures, ectopic mitotic figures and to macrophage-like cells, respectively. The brackets in* **(h)** *encompass the optic nerve coloboma and the squared brackets in* **(e and i)** *the equatorial region of the lens. The asterisks indicate artifactual detachments generated during tissue processing. Magnifications: a,b,e and f: x43; c,d: x430; g,h: x86; i,j: x178.*

lost the ability to express RARβ (reviewed in Lotan, 1993) and that RARβ (or RARβ2) plays a role in retinoic acid-induced apoptosis and/or growth arrest in HeLa cells and breast cancer cells (Seewaldt *et al.*, 1995; Liu *et al.*, 1996; Si *et al.*, 1996), have suggested that RARβ could be involved in mechanisms preventing cell transformation. In this respect, our present finding that RARβ is involved in cell death and/or proliferation of a subset of embryonic fibroblasts is of interest, and further investigations on these cells in cultures may provide insight into some aspects of retinoid action on cell fate.

Morphometric analysis of the palpebral aperture in E14.5 fetuses reveals that all 3 RAR isotypes are involved in its formation. Interestingly, RARs are also required for eyelid fusion, as all Aα/Aγ mutants and about one third of the Aα1/Aα2$^{+/-}$/Aγ mutants are born with open eyes (Lohnes *et al.*, 1994). The RA-dependence of both eyelid formation and fusion is further supported by the retinoic acid-rescue of lidgap mutations (i.e. mutations which cause the defect of open eye at birth): normal eyelid development can be restored in lidgap mouse mutants by maternal treatment with retinoic acid either at E11.5 (i.e. just prior to the onset of eyelid formation) or E14.5 (just prior to the onset of eyelid closure) (Juriloff and Harris, 1993).

Eye development results from cell interactions between two epithelia, the ectoderm and neurectoderm, and a NCC-derived mesenchyme (Johnston *et al.*, 1979 and references therein). All of these structures are affected to some extent in Aβ/Aγ mutants; therefore, as it is often the case when combination of multiple abnormalities exists within the same organ system, it is difficult to identify the primary and secondary target tissue(s) of this double mutation. The periocular mesenchyme might be a primary target, since it exhibits high levels of both RARβ and RARγ proteins and/or transcripts from E12.5 until after birth (Dollé *et al.*, 1989; Grondona *et al.*, 1996; see also PO in Fig. 10a and c), and it also expresses high levels of RALDH2 (Niederheither *et al.*, 1997) a RA-generating dehydrogenase (Zhao *et al.*, 1996). Thus, the periocular mesenchyme may be both a possible source of RA and a target for a RA autocrine action. In this respect, we note that all of its derivatives are consistently affected in the Aβ/Aγ mutants. It is more difficult to account for the occurrence of a shortening of the ventral retinal field and of a pre-natal retinal dysplasia in Aβ/Aγ mutants, since the possible role of the periocular mesenchyme in retinal patterning is not documented, and RARγ as well as RARβ are apparently absent from the pre-natal neural retina (see RE, ONL and GCL in Fig. 10a and c). Interestingly, Aβ2/Aγ2 mutants develop post-natally a completely different form of retinal dysplasia probably secondary to RPE defects (Grondona *et al.*, 1996).

Limb development

3 RARs are expressed in the interdigital mesenchyme during the period of morphogenetic cell death (Dollé *et al.*, 1989; Ruberte *et al.*, 1990; Fig. 6a-c) and RA has been shown to induce digit separation in cultured embryonic limbs (Lussier *et al.*, 1993). The interdigital webbing observed in ~10% of RARγ mice affects the interzones between digits 2-3 and/or 3-4 in the hindlimbs and is exceptional in forelimbs (Lohnes *et al.*, 1993; Kastner *et al.*, 1997). Interdigital webbing is also seen in some RARα mutants (Lufkin *et al.*, 1993) and is never found in RARβ mutants (present report). Our observation that Aβ/Aγ and Aβ$^{+/-}$/Aγ mutant mice display a severe and completely penetrant interdigital webbing strengthen the conclusion that RA plays a critical role in the separation of the digits. By an irony of fate, this role of RA was originally inferred from the distribution pattern of RARβ (Dollé *et al.*, 1989) whose inactivation has no effect on interdigital tissues. Our data also demonstrate that the interdigital webbing induced by RAR inactivations is due to a lack of involution of the fetal interdigital mesenchyme, not to a post-natal failure of breakdown of the epithelial lamina normally connecting the digits at birth. Interestingly, soft tissue syndactyly was recently observed following inhibition of BMP (Bone Morphogenetic Protein) expression in the chick limb bud (Zou and Niswander, 1996). Our compound mutants of RARβ and RARγ should represent useful tools with which to investigate the relationships between the RA and BMP signaling pathways in controlling interdigital cell death.

Cranial development and atavistic traits

Besides the dramatic craniofacial skeletal deficiencies seen in Aα/Aγ mutants (Lohnes *et al.*, 1994), more subtle defects which often alter the shape of a single skeletal piece are observed in Aα, Aγ, Aα1/Aγ, Aα/Aβ2, Aα/Aβ, Aβ2/Aγ and Aβ/Aγ mice, including: a cartilaginous or osseous connection between the incus middle ear bone and the alisphenoid bone (pterygoquadrate element); a medial cartilaginous wall for the cavum epipterycum (pila antotica); malformation of the squamosal bone; agenesis of the rostral ethmoturbinate and maxillary sinus; and absence of the metoptic pillar (Lohnes *et al.*, 1994 and present report). The pterygoquadrate element and pila antotica, which were lost during evolution from reptiles to mammals, may represent atavistic features (discussed in Mark *et al.*, 1995). Along the same lines, ethmoturbinate bones and paranasal sinuses (such as the maxillary sinus) are typical mammalian features not present in reptiles (Novacek, 1993). Thus, their absence in Aβ/Aγ mutants could also mimick an atavistic condition. The pila metoptica is absent in monotremes and marsupials, but present in placental mammals, as well as in the reptilian ancestors of mammals. Therefore, the absence of this structure in Aγ null mutants and compound mutants of RARγ and RARβ cannot be interpreted as an atavism. However, it further suggests that changes in the temporal or spatial patterns of expression of RARs may have provided a general mechanism for modifying the number and morphology of individual cranial skeletal elements during vertebrate evolution. Interestingly, such a function has also been assigned to members of the BMP family (reviewed by Kingsley, 1994; Hogan, 1996). Thus, BMPs which can elicit ectopic bone formation, possibly by promoting the entry of multipotent stem cells into the chondrogenic pathway, and whose loss-of-function mutations result in the disruption of specific subsets of skeletal elements could mediate the effects of RA on cranial skeletal patterning.

The PHPV, which is homologous to the reptilian pecten oculi, and the shortening of the ventral retina (Kastner *et al.*, 1994) may also represent atavistic traits.

Axial specification

It was previously demonstrated that RARγ and (to a lesser extent) RARα are important for patterning of the body anteroposterior axis (Lohnes *et al.*, 1993; Lufkin *et al.*, 1993). RARβ also appears to be involved in this process, as RARβ single mutants and compound mutants of RARβ and either RARα or RARγ display homeotic transformations or malformations of vertebrae. The penetrance and expressivity of some of these defects increase in a graded manner with subsequent loss of the other RAR alleles from the RARβ null background, indicating that the specification of the affected segments could be particularly sensitive to RAR gene

dosage effects. Most of the vertebral abnormalities observed in the RAR mutants probably arise through altered expression of some *Hox* genes (discussed in Lohnes *et al.*, 1994; Kastner *et al.*, 1997). That RARβ transcripts were never detected during mouse development in presomitic mesoderm, somites or sclerotomes, while present in neurectoderm (Dollé *et al.*, 1990; Ruberte *et al.*, 1991), suggests that the effect of RARβ on vertebral morphogenesis could involve RA-dependent diffusible signals emanating from the neural tube (Pourquié *et al.*, 1993).

Specificity and functional redundancy

In the early 90's, it was expected that systematic gene knock-out in the mouse would lead to defined abnormal phenotypes, and thus allow to uncover the functional domain of given genes. There are now numerous examples where this expectation was not fulfilled, either because the mutation resulted in a lethal phenotype, or because of genetic redundancies. Two genes are redundant whenever their respective products can perform equivalent functions. The possession of two fully redundant genes is, in an evolutionary sense, unlikely. Thus, the finding of apparently 'dispensable' genes (i.e. genes whose inactivation has no apparent phenotypic consequences) must correspond to the lack of precision of the phenotypic test by which mutants are deemed to be asymptomatic, and/or to the fact that the sample size might be too small to detect a small fitness reduction of the mutants, and/or to the fact that the fitness disadvantage might be manifested only in environments that are not duplicated in the laboratory (Brookfield, 1992; Thomas, 1993; Gabor-Miklos and Rubin, 1996). Along this line, it is noteworthy that the PHPV present in RARβ2 (Grondona *et al.*, 1996) and RARβ (present report) null mutants was first overlooked due to its incomplete penetrance and lack of manifestation on the behavior of the mutants in the animal facility (Mendelsohn *et al.*, 1994c; Luo *et al.*, 1995). However, it does result in a very poor vision (see Reese, 1955) which, *per se*, is obviously sufficient to account for the evolutionary conservation of the RARβ2 isoform.

A classical genetic test for redundancy between two gene products *in vivo* is to determine whether compound loss-of-function mutants display novel abnormalities compared to single mutants or show an increase in the penetrance and/or expressivity of a phenotype already present in the single mutant(s) (Thomas, 1993). However, the phenotypic redundancy observed in RAR/RAR compound mutants (and to a much lesser extent in RXRα/RAR compound mutants; Kastner *et al.*, 1997) should not be taken as an absolute proof of functional redundancy. Other explanations cannot be excluded, notably: 1) action of distinct RARs on a specific subset of target genes within the same cell; 2) action of distinct RARs in different tissues whose reciprocal interactions are normally required for the making of a given structure. This second possibility is particularly appealing in structures which display developmental defects in Aβ/Aγ mutants, although showing clearly non-overlapping patterns of RARβ and RARγ expression such as the interdigital soft tissue and the ethmoturbinates. In this latter localization, RARγ is expressed in the maturing cartilage (e.g. E1 in Fig. 10b) whereas RARβ transcripts are confined to the perichondrium (PC in Fig. 10b).

The phenomenon of functional redundancy observed in RAR knockout experiments might indicate that, in certain organ systems, all RARs (in the form of heterodimers with RXRα; Kastner *et al.*, 1997) are able to transactivate with similar efficiencies most of the RA target genes. The only requirement for normal development would be to reach a critical level of RXRα-RAR heterodimers in a given cell at a given time of its ontogeny. This possibility is discussed below in the case of the mesectodermal cells of the eyelid anlagen. Alternatively, the phenomenon of functional redundancy may not reflect a lack of functional specificity of RARs in the WT situation, but merely indicates the existence of compensatory mechanisms operating essentially, if not exclusively, in the artifactual context of the single null mutants. This second scenario might apply to the RA-mediated events which are required for the involution of the primary vitreous body and for the morphogenesis of the Harderian gland.

A mild reduction of the palpebral aperture is present in Aα, $A\beta^{+/-}$ and $A\gamma^{+/-}$ single mutants; additive effects of RAR mutations on the size of the palpebral aperture are observed in compound heterozygotes (as well as $A\alpha/A\beta^{+/-}$ and $A\alpha^{+/-}/A\beta$ mutants), and disrupting only one allele of either RARβ or RARγ in the Aγ or Aβ null genetic backgrounds leads to synergistic effects. As RARα, RARβ and RARγ are all strongly expressed in the mesenchymal component of the eyelid anlagen at the onset of their formation (E in Fig. 10a), a decrease in the total intracellular amount of RARs represents the simplest explanation to account for the appearance of a blepharophimosis in some mutants.

On the other hand, several lines of evidence support the conclusion that, although the PHPV is completely penetrant in compound mutants only (e.g. Aα/Aβ and Aβ/Aγ mutants), RARβ is the receptor specifically involved in the disappearance of the primary vitreous body. Firstly, in the primary vitreous body RARβ transcripts are, by far, the most abundant; RARα and RARγ transcripts are not detected above background level in this structure (Fig. 10a). Secondly, a PHPV is observed with a high frequency only in RARβ (and RARβ2) null mutant mice; its presence in RARγ null mice is similar to that in WT mice and it is not detected in RARα null mice nor in Aα1/Aα2+/-/Aγ mice (Lohnes *et al.*, 1994), Aα/Aγ1 or Aα/Aγ2 mice (V. Subbarayan, P. Kastner, M.M.P. Gorry, and P.C., unpublished results). Note also that the PHPV in Aα/Aγ mice is most likely secondary to retinal colobomas (as discussed in Lohnes *et al.*, 1994). The third argument supporting a unique role of RARβ in the disappearance of the primary vitreous stems from the observation of mice in which half the RXRα/RAR heterodimers (the functional units of the retinoid signaling pathway) have been inactivated: ~50% of the $A\beta^{+/-}/X\alpha^{+/-}$ mice display a PHPV (Kastner *et al.*, 1997), whereas this abnormality is never observed in $A\gamma^{+/-}/X\alpha^{+/-}$ mice (our personal observation). That the PHPV is not observed in ~15% of the RARβ null mutants is most easily explained by a functional compensation involving mainly (if not exclusively) RARγ: in $A\beta^{+/-}/A\gamma$ the PHPV is fully penetrant; in contrast, $A\alpha/A\beta^{+/-}$ mice do not display this abnormality. Finally, that the PHPV is highly penetrant in compound mutants with only one allele of the RARβ gene disrupted (i.e. $A\beta^{+/-}/X\alpha^{+/-}$, $A\beta^{+/-}/A\gamma^{-/-}$, $A\beta^{+/-}/A\gamma^{+/-}$) supports the conclusion that, in 'real life' (the WT mice), a full complement of the RARβ gene is required for the involution of the primary vitreous.

Along the same lines, RARγ is most probably the only RAR involved in the morphogenesis of the Harderian gland, despite the low penetrance of its agenesis in RARγ null mutants (Lohnes *et al.*, 1993, and present report). Firstly, this defect is fully penetrant in Aα1/Aγ, Aβ2/Aγ and Aβ/Aγ mutants but never observed in Aα/Aβ mutants (Lohnes *et al.*, 1994 and present results). Secondly, only RARγ transcripts are present at apparently high levels in the

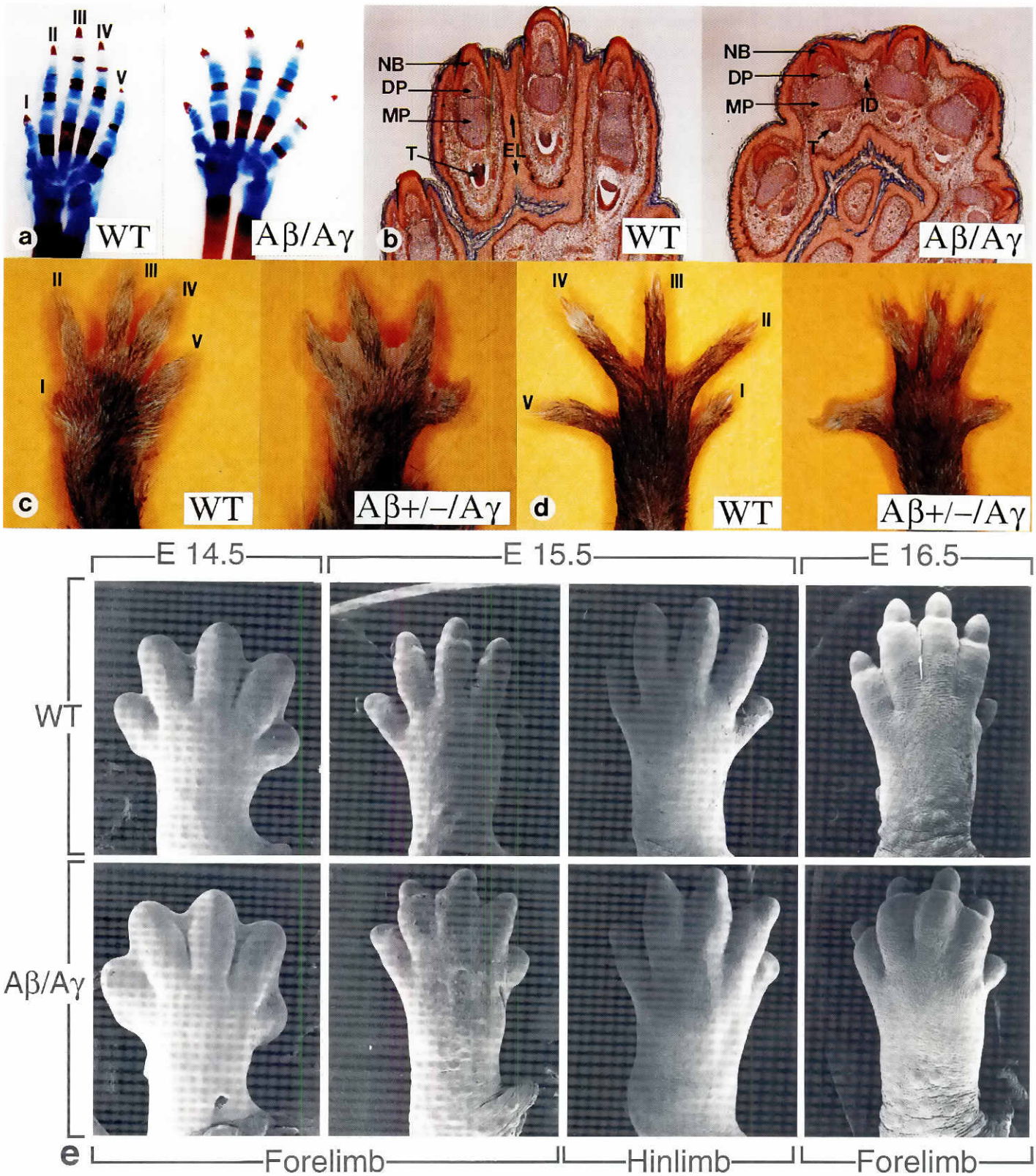

Fig. 9. Failure of digit separation and soft tissue syndactyly in compound mutants of RARβ and RARγ (genotypes as indicated). (a) *Dorsal views of E18.5 forelimbs.* **(b)** *Histological sections through E18.5 forelimbs.* **(c)** *Forelimbs and* **(d)** *hindlimb of 6 week-old mice.* **(e)** *Scanning electron micrographs. I-V: digits; DP, distal phalanx; EL, epithelial lamina connecting the digits; ID, persistent interdigital mesenchyme; MP, medial phalanx; NB, nail bed; T, tendon; the small white arrow in (e) indicates an interdigital epithelial ridge. Magnifications: b: x26; x18 (e; E14.5) and x13 (e; E15.5 and 16.5).*

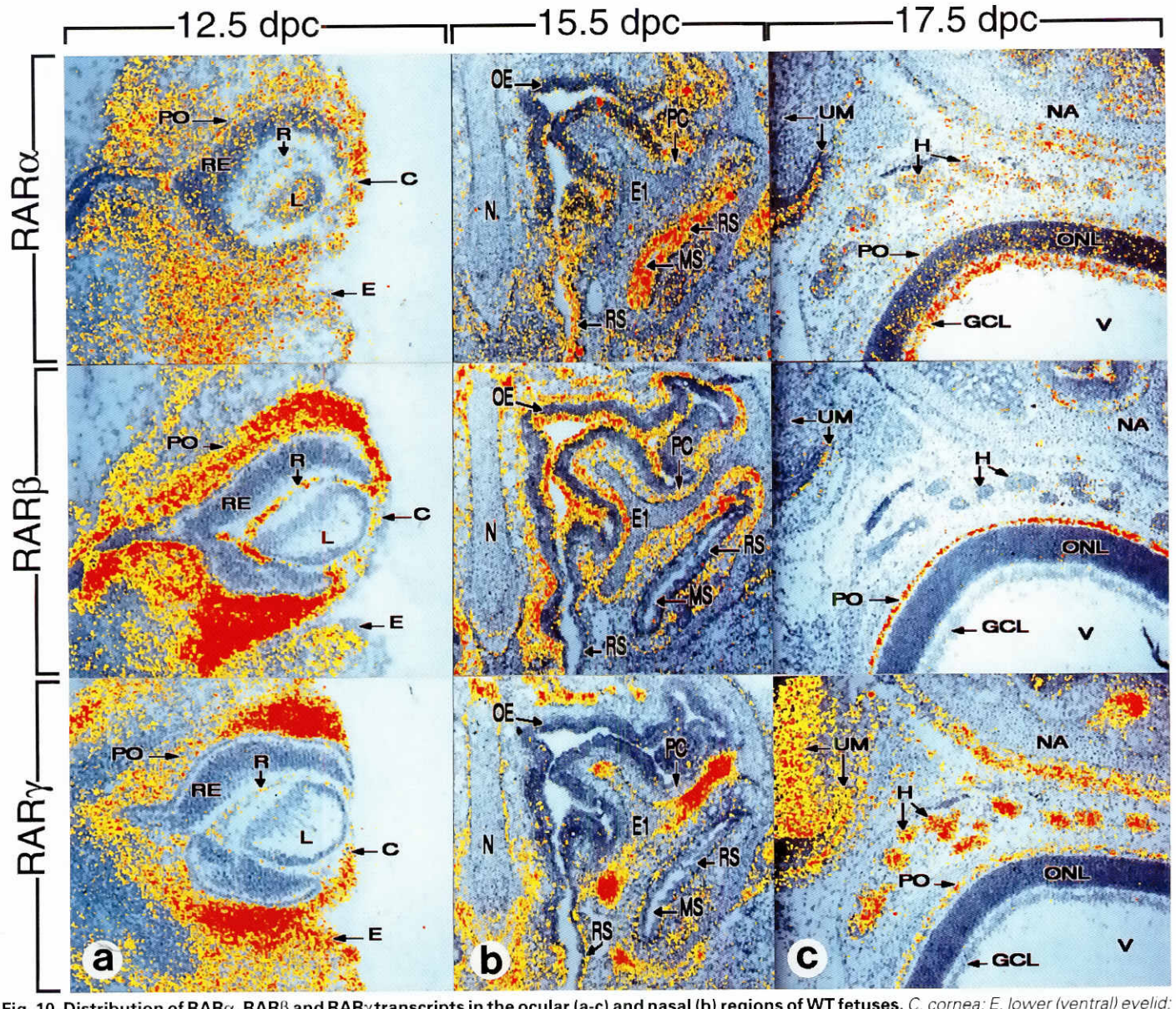

Fig. 10. Distribution of RARα, RARβ and RARγ transcripts in the ocular (a-c) and nasal (b) regions of WT fetuses. *C, cornea; E, lower (ventral) eyelid; E1, rostral ethmoturbinate; GCL, ganglion cell layer; H, epithelial portion of the Harderian gland; L, lens; MS, maxillary sinus; N, nasal septum; NA, nasal capsule; OE, olfactory epithelium; ONL, outer nuclear layer; PC, perichondrium; PO, periocular mesenchyme; R, primary vitreous body; RE, retina; RS, respiratory epithelium; UM, first upper molar; V, secondary vitreous body. The in situ hybridization signal is shown in false colors after computer processing of a bright-field view (showing the histology) and of a dark field view (revealing the autoradiography silver grain signal) of the same section. The threshold levels for false colors have been selected in order to eliminate the isolated (background) silver grains, but to reveal all significant labeling (yellow) as well as more intensely labeled areas (red). Magnification: a: x45; b,c: x36.*

epithelial component of the developing Harderian gland (H in Fig. 10c); in contrast *in situ* hybridization failed to detect RARβ expression in both the Harderian gland epithelium and mesenchyme (Fig. 10c) and revealed only a weak expression of RARα (Fig. 10c). Thus, it appears that the absence of RARγ in the Harderian gland can be functionally compensated by RARα1 and RARβ2 (Lohnes *et al.*, 1994), but it is unlikely that RARα and RARβ are actually involved in the formation of this structure in WT animals. Note in addition that, although RARβ expression could not be detected in the Harderian gland, it can nevertheless partially compensate for the loss of RARγ in this structure. This emphasizes the lack of sensitivity of the available *in situ* detection techniques.

In any event, the present study, together with recent studies carried out with F9 cells (Taneja *et al.*, 1996) and RXRα/RAR compound mutant mice (Kastner *et al.*, 1994 and 1997) further support the possibility that the functional redundancies inferred from the morphological analysis of mice bearing mutations in the different RAR isotypes might reflect artifactual situations generated by the knock-out.

Materials and Methods

Targeting vector and homologous recombination

Genomic clones for the mouse RARβ (mRARβ) locus were obtained by screening a genomic library established in λEMBL3 from 129/Sv mouse DNA with a mRARβ cDNA probe (Zelent *et al.*, 1991). To construct the targeting vector, a 3.5kb SalI-HindIII genomic fragment containing exons E9 to E11 was first inserted into pTZ18R plasmid (Pharmacia). Subsequently, the 1.3kb BglII fragment containing E9 and most part of E10 was replaced with a PGK-Neo cassette (Adra *et al.*, 1987). A 3.5kb HindIII-SalI genomic fragment containing E8 was then introduced 5' to this construct and the resulting 7kb HindIII DNA fragment was subsequently cloned into a Bluescript plasmid (pBSII-SK+, Stratagene) harboring an Herpes simplex virus thymidine kinase gene (HSV-TK; Lufkin *et al.*, 1991). The linearized final plasmid was electroporated into D3 embryonic stem (ES) cells (Gossler *et al.*, 1986; Lufkin *et al.*, 1991). After selection, resistant clones were expanded. Genomic DNA was prepared from each clone and analyzed by Southern blotting with probes A (Fig. 1b). The positive clone XW98 was injected into C57BL/6 blastocysts, and the resulting male chimeras tested for germline transmission.

Mice

All the mice used in the present study were on a mixed 129/Sv· C57BL/6 genetic background. RARβ null mutants and RARβ/RARα or RARβ/RARγ double null mutants were produced from the intercrosses of RARβ$^{+/-}$ and RARβ/RARα or RARβ/RARγ double heterozygotic mice, respectively. Noon of the day of a vaginal plug was taken as 0.5 day post-coitum (E0.5). Embryos were collected by cesarian section and the yolk sacs were taken for DNA extraction. Genotypes were determined by Southern blotting. Genotyping conditions for RARα and RARγ mutant mice have been described previously (Lohnes *et al.*, 1993; Lufkin *et al.*, 1993).

RNAse protection analysis

Total RNA was prepared from E13.5 embryos (Chomczynski and Sacchi, 1987) . Approximately 50 μg of total RNA was used per hybridization at 55°C. The conditions for the preparation of probes and hybridization reactions were essentially as described by Ausubel *et al.* (1987). Template for synthesis of the RARβ riboprobe was obtained by subcloning the EcoRV-EcoRI fragment of mRARβ cDNA containing most part of the ligand binding domain (Zelent *et al.*, 1991). The RARα2 probe included the A2 region through the RARα C region to generate protected fragments of 382 nt for RARα2 and 179 nt for RARα1 (Lufkin *et al.*, 1993). The RARγ2 probe spanned the A2 region through the C region to generate protected fragments of 368 nt for RARγ2 and 162 nt for RARγ1 (Lohnes *et al.*, 1993). The histone antisense riboprobe used as an internal control generate a 130 nt RNA fragment (a gift from R. Grosschedl, Howard Hughes Medical Institute, San Francisco, USA).

Protein analysis

Cytoplasmic and nuclear protein extracts were prepared from E10.5 WT, heterozygous and homozygous RARβ mutant embryos according to Rochette-Egly *et al.* (1991). Whole cell extracts from transfected Cos-1 cells were prepared as described (Gaub *et al.*, 1992). The proteins (20 μg for cytosolic extracts and 80 μg for nuclear extracts) were separated by SDS-PAGE and transferred to nitrocellulose membrane. Immunodetection procedures were as described previously (Rochette-Egly *et al.*, 1991) using as antibody preparations rabbit polyclonal antisera specific for RARα [RPα(F), Gaub *et al.*, 1992], RARβ [RPβ(F)2, Rochette-Egly *et al.*, 1992] and RARγ [RPγ(mF), raised against synthetic peptide SP288 (amino acids 427-455)]. Monoclonal antibodies specific for CRABP-I (3CRA10F5) and CRABP-II (1CRA4C9) were also used (Lampron *et al.*, 1995). Immunoreactions were visualized using protein A or anti-mouse immunoglobulins coupled to horseradish peroxidase, followed by chemiluminescence according to the manufacturer's protocol (Amersham).

Histological and skeletal analyses

Serial histological sections were stained with Groat's hematoxylin and Mallory's trichrome and skeletons with alcian blue and alizarin red as previously described (Lufkin *et al.*, 1991; Mark *et al.*, 1993).

Histochemistry, immunochemistry and in situ hybridization

Acetylcholinesterase activity in brain section was detected according to Paxinos and Watson (1986). Whole-mount anti-neurofilament immunostaining and *in situ* hybridization on frozen tissue sections were performed as previously described (Mark *et al.*, 1993; Décimo *et al.*, 1995). For RAR immunolocalization studies, 10 μm thick frozen tissue sections were fixed in Zamboni's fluid (2% paraformaldehyde, 0.21% picric acid in 0.15M sodium phosphate buffer, pH 7.3), rinsed in PBS – 0.05% Tween 20 (PBS-T) to block unspecific binding (30 min at 24°C). The sections were then incubated with the purified rabbit polyclonal antibodies diluted in PBS-T plus goat serum for 1 h at 24°C. These antisera were purified by precipitation with ammonium sulfate and application onto sulfolink gel columns (Pierce, USA) coupled with the corresponding synthetic peptides. After rinsing in PBS-T (3x5 min) the bound antibodies were revealed using an ABC system (Vector) according to the manufacturer's instructions. Tissues from RARα, RARβ or RARγ null mutants were used as negative controls of the immunostaining procedure (e.g. in Fig. 6f).

Acknowledgments

We are grateful to P. Gorry and P. Kastner for RARα and RARγ mutant mice, M.P. Gaub for antibodies, P. Kastner and C. Mendelsohn for RARα, RARγ riboprobes and RARβ cDNA. We are also grateful to M. Le Meur for her collaboration, Dr R. Kemler for the gift of D3 ES cells, T. Lufkin and D. Lohnes for the PGK Neo and HSV-TK cassettes, V. Vivat for advice in transfection experiments and J. Grondona for help in dissecting some eyes. The 2H3 hybridoma was obtained from the Developmental Studies Hybridoma Bank maintained by the Department of Pharmacology and Molecular Sciences, Johns Hopkins University School of Medicine, Baltimore, MD and the Department of Biology, University of Iowa, Iowa City, IA, under contract N01-HD-6-2915 from the NICHD. We thank B. Bondeau, B. Weber, C. Fischer, V. Giroult, S. Heyberger, C. Birling, M. Digelmann, J.M. Kuhry, D. Queuche as well as the staff from the microinjection, and animal facilities for excellent technical assistance. We also thank J.L. Vonesh, B. Boulay, J.M. Lafontaine and the secretarial staff for their help in the preparation of this manuscript. This work was supported by funds from the Centre National de la Recherche Scientifique (CNRS), the Institut National de la Santé et de la Recherche Médicale (INSERM), the Centre Hospitalier Régional Universitaire, the Collège de France, the Association pour la Recherche sur le Cancer (ARC), the Human Frontier Science Program, and Bristol Myers Squibb.

References

ADRA, C.N., BŒR, P.H. and McBURNEY, M.W. (1987). Cloning and expression of the mouse pgk-1 gene and the nucleotide sequence of its promoter. *Gene 60:* 65-74.

AUSUBEL, F.M., BRENT, R., KINGSTON, R.E., MOORE, D.D., SEIDMAN, J.G., SMITH, J.A. and STRUHL, K. (1987). *Current Protocols in Molecular Biology.* Green Pub. Assoc. and Wiley-Interscience. Wiley, New York.

BARISHAK, Y.R. (1992). *Embryology of the Eye and Its Adnexae.* Karger, Basel.

BEDO, G., SANTISTEBAN, P. and ARANDA, A. (1989). Retinoic acid regulates growth hormone gene expression. *Nature 339:* 231-234.

BLOMHOFF, R. (1994). *Vitamin A in Health and Disease.* Marcel Dekker, New York.

BOCKMAN, D.E. and KIRBY, M.L. (1984). Dependence of thymus development on derivatives of the neural crest. *Science 223:* 498-500.

BROOKFIELD, J. (1992). Can gene be truly redundant ? *Curr. Biol. 2:* 553-554.

CAPECCHI, M.R. (1989). Altering the genome by homologous recombination. *Science 244:* 1288-1292.

CHAMBON, P. (1996). A decade of molecular biology of retinoic acid receptors. *FASEB J. 10:* 940-954.

CHOMCZYNSKI, P. and SACCHI, N. (1987). Single-step method of RNA isolation by acid guanidinium thiocyanate-phenol-chloroform extraction. *Anal. Biochem. 162:* 156-159.

DÉCIMO, D., GEORGES-LABOUESSE, E. and DOLLÉ, P. (1995). *In situ* hybridization of nucleic acid probes to cellular RNA. In *Gene Probes, A Practical Approach Book,* Vol. II (Eds. B.D. Hames and S. Higgins), pp. 183-210.

DIAMOND, M.K. (1989). Coarctation of the stapedial artery: an unusual adaptive response to competing functional demands in the middle ear of some eutherians. *J. Morphol. 200:* 71-86.

DOLLÉ, P., RUBERTE, E., KASTNER, P., PETKOVICH, M., STONER, C.M., GUDAS, L.J. and CHAMBON, P. (1989). Differential expression of genes encoding alpha, beta and gamma retinoic acid receptors and CRABP in the developing limbs of the mouse. *Nature 342:* 702-705.

DOLLÉ, P., RUBERTE, E., LEROY, P., MORRISS-KAY, G. and CHAMBON, P. (1990). Retinoic acid receptors and cellular retinoid binding proteins. I. A systematic study of their differential pattern of transcription during mouse organogenesis. *Development 110:* 1133-1151.

FOLKERS, G.E., VAN DER LEEDE, B.J.M. and VAN DER SAAG, P.T. (1993). The retinoic acid receptor-β2 contains two separate cell-specific transactivation domains, at the N-terminus and in the ligand-binding domain. *Mol. Endocrinol. 7:* 616-627.

GABOR-MIKLOS, G.L. and RUBIN, G.M. (1996). The role of the genome project in determining gene function: insights from model organisms. *Cell 86:* 521-529.

GAUB, M.P., ROCHETTE-EGLY, C., LUTZ, Y., ALI, S., MATTHES, H., SCHEUER, I. and CHAMBON, P. (1992). Immunodetection of multiple species of retinoic acid receptor alpha: evidence for phosphorylation. *Exp. Cell Res. 201:* 335-346.

GOSSLER, A., DŒTSCHMAN, T., KORN, R., SERFLING, E. and KEMLER, R. (1986). Transgenesis by means of blastocyst-derived embryonic stem cell lines. *Proc. Natl. Acad. Sci. USA 83:* 9056-9069.

GRAY, S.W. and SKANDALAKIS, J.E. (1972). *Embryology for Surgeons. The Embryological Basis for the Treatment of Congenital Defects.* Saunders Co, Philadelphia.

GRONDONA J.M., KASTNER, P., GANSMULLER, A., DÉCIMO, D., CHAMBON, P. and MARK, M. (1996). Retinal dysplasia and degeneration in RARβ2/RARγ2 compound mutant mice. *Development 122:* 2173-2188.

HARRIS, M.J. and McLEOD, M.J. (1982). Eyelid growth and fusion in fetal mice. *Anat. Embryol. 164:* 207-220.

HOGAN, B.L.M. (1996). Bone morphogenetic proteins: multifunctional regulators of vertebrate development. *Genes Dev. 10:* 1580-1594.

JIANG, H., SOPRANO, D.R., LI, S.W., SOPRANO, K.J., PENNER, J.D., GYDA III, M. and KOCHHAR, D.M. (1995). Modulation of limb bud chondrogenesis by retinoic acid and retinoic acid receptors. *Int. J. Dev. Biol. 39:* 617-627.

JOHNSTON, M.C., NODEN, D.M., HAZELTON, R.D., COULOMBRE, J.L. and COULOMBRE, A.J. (1979). Origins of avian ocular and periocular tissues. *Exp. Eye Res. 29:* 27-43.

JURILOFF, D.M. and HARRIS, M.J. (1993). Retinoic acid, cortisone, or thyroxine suppresses the mutant phenotype of the eyelid development mutation, Ig^{MI}, in mice. *J. Exp. Zool. 265:* 144-152.

KASTNER, P., GRONDONA, J.M., MARK, M., GANSMULLER, A., LEMEUR, M., DÉCIMO, D., VONESCH, J.L., DOLLE, P. and CHAMBON, P. (1994). Genetic analysis of RXRα developmental function: convergence of RXR and RAR signalling pathways in heart and eye morphogenesis. *Cell 78:* 987-1003.

KASTNER, P., MARK, M. and CHAMBON, P. (1995). Nonsteroid nuclear receptors: what are genetic studies telling us about their role in real life? *Cell 83:* 859-869.

KASTNER, P., MARK, M., GHYSELINCK, N.B., KREZEL, W., DUPÉ, V., GRONDONA, J.M. and CHAMBON, P. (1997). Genetic evidence that the retinoid signal is transduced by heterodimeric RXR/RAR functional units during mouse development. *Development 124:* 313-326.

KINGSLEY, D.M. (1994). What do BMPs do in mammals? Clues from the mouse short-ear mutation. *Trends Genet. 10:* 16-21.

LAMPRON, C., ROCHETTE-EGLY, C., GORRY, P., DOLLÉ, P., MARK, M., LUFKIN, T. LEMEUR, M. and CHAMBON, P. (1995). Mice deficient in cellular retinoic acid binding protein II (CRABP-II) or in both CRABP-I and CRAPB-II are essentially normal. *Development 121:* 539-548.

LANG, R.A. and BISHOP, J.M. (1993). Macrophages are required for cell death and tissue remodeling in the developing mouse eye. *Cell 74:* 453-462.

LIU, Y., LEE, M.O., WANG, H.G., LI, Y., HASHIMOTO, Y., KLAUS, M., REED, J.C. and ZHANG X.K. (1996). Retinoic acid receptor β mediates the growth inhibitory effect of retinoic acid by promoting apoptosis in human breast cancer cells. *Mol. Cell. Biol. 16:* 1138-1149.

LOHNES, D., KASTNER, P., DIERICH, A., MARK, M., LE MEUR, M. and CHAMBON, P. (1993). Function of retinoic acid receptor gamma in the mouse. *Cell 73:* 643-658.

LOHNES, D., MARK, M., MENDELSOHN, C., DOLLÉ, P., DIERICH, A., GORRY, P., GANSMULLER, A. and CHAMBON, P. (1994). Function of the retinoic acid receptors (RARs) during development (I). Craniofacial and skeletal abnormalities in RAR double mutants. *Development 120:* 2723-2748.

LOTAN, R. (1993). Squamous differentiation markers in normal, premalignant, and malignant epithelium: effects of retinoids. *J. Cell Biochem. 17 (Suppl.):* 167-174.

LUFKIN, T., DIERICH, A., LE MEUR, M., MARK, M. and CHAMBON, P. (1991). Disruption of the Hox-1.6 homeobox gene results in defects in a region corresponding to its rostral domain of expression. *Cell 66:* 1105-1119.

LUFKIN, T., LOHNES, D., MARK, M., DIERICH, A., GORRY, P., GAUB, M.P., LE MEUR, M. and CHAMBON, P. (1993). High postnatal lethality and testis degeneration in retinoic acid receptor alpha mutant mice. *Proc. Natl. Acad. Sci. USA 90:* 7225-7229.

LUO, J., PASCERI, P., CONLON, R.A., ROSSANT, J. and GIGUERE, V. (1995). Mice lacking all isoforms of retinoic acid receptor beta develop normally and are susceptible to the teratogenic effects of retinoic acid. *Mech. Dev. 53:* 61-71.

LUO, J., SUCOV, H.M., BADER, J.A., EVANS, R.M. and GIGUÈRE, V. (1996). Compound mutants for retinoic acid receptor (RAR) β and RARα1 reveal developmental functions for multiple RARβ isoforms. *Mech. Dev. 55:* 33-44.

LUSSIER, M., CANOUN, C., MA, C., SANK, A. and SHULER, C. (1993). Interdigital soft tissue separation induced by retinoic acid in mouse limbs cultured *in vitro*. *Int. J. Dev. Biol. 37:* 555-564.

MACONNACHIE, E. (1979). A study of digit fusion in the mouse embryo. *J. Embryol. Exp. Morphol. 49:* 259-276.

MANGELSDORF, D.J. and EVANS, R.M. (1995). The RXR heterodimers and orphan receptors. *Cell 83:* 841-850.

MARK, M., LOHNES, D., MENDELSOHN, C., DUPÉ, V., VONESCH, J.L., KASTNER, P., RIJLI, F., BLOCH-ZUPAN, A. and CHAMBON, P. (1995). Roles of retinoic acid receptors and of Hox genes in the patterning of the teeth and of the jaw skeleton. *Int. J. Dev. Biol. 39:* 111-121.

MARK, M., LUFKIN, T., VONESCH, J.L., RUBERTE, E., OLIVO, J.C., DOLLE, P., GORRY, P. LUMSDEN, A., and CHAMBON, P. (1993). Two rhombomeres are altered in Hoxa-1 mutant mice. *Development 119:* 319-338.

MENDELSOHN, C., LARKIN, S., MARK, M., LE MEUR, M., CLIFFORD, J., ZELENT, A. and CHAMBON, P. (1994a). RAR beta isoforms: distinct transcriptional control by retinoic acid and specific spatial patterns of promoter activity during mouse embryonic development. *Mech. Dev. 45:* 227-241.

MENDELSOHN, C., LOHNES, D., DECIMO, D., LUFKIN, T., LE MEUR, M., CHAMBON, P. and MARK, M. (1994b). Function of the retinoic acid receptors (RARs) during development (II). Multiple abnormalities at various stages of organogenesis in RAR double mutants. *Development 120:* 2749-2771.

MENDELSOHN, C., MARK, M., DOLLÉ, P., DIERICH, A., GAUB, M.P., KRUST, A., LAMPRON, C. and CHAMBON, P. (1994c). Retinoic acid receptor beta 2 (RAR beta 2) null mutant mice appear normal. *Dev. Biol. 166:* 246-258.

MENDELSOHN, C., RUBERTE, E., LE MEUR, M., MORRISS-KAY, G. and CHAMBON, P. (1991). Developmental analysis of the retinoic acid-inducible RARβ2 promoter in transgenic animals. *Development 113:* 723-734.

NAGPAL, S., ZELENT, A. and CHAMBON, P. (1992). RARβ4, a retinoic acid receptor isoform is generated from RARβ2 by alternative splicing and usage of a CUG initiator codon. *Proc. Natl. Acad. Sci. USA 89:* 2718-2722.

NIEDERREITHER, K., McCAFFERY, P., DRÄGER, U.C., CHAMBON, P. and DOLLÉ, P. (1997). Restricted expression and retinoic acid-induced downregulation of the retinaldehyde dehydrogenase type 2 (RALDH-2) gene during mouse development. *Mech. Dev. 62:* 67-78.

NOVACEK, M.J. (1993). Patterns of diversity in the mammalian skull. In *The Skull,* Vol. 2 (Eds. J. Hanken and B.K. Hall). The University of Chicago Press, Chicago, pp. 438-548.

PAXINOS, G. and WATSON, C. (1986). *The Rat Brain in Stereotaxic Coordinates.* Academic Press, San Diego.

POURQUIÉ, O., COLTEY, M., TEILLET, M.A., ORDAHI, C. and LE DOUARIN, N.M. (1993). Control of dorsoventral patterning of somitic derivatives by notochord and floor plate. *Proc. Natl. Acad. Sci. USA 90:* 5242-5246.

REESE, A.B. (1955). Persistent hyperplastic primary vitreous. *Am. J. Ophthalmol. 40:* 317-331.

RENAUD, J.P., ROCHEL, N., RUFF, M., VIVAT, V., CHAMBON, P., GRONEMEYER, H. and MORAS, D. (1995). Crystal structure of the RAR-γ ligand-binding domain bound to all-trans retinoic acid. *Nature 378:* 681-689.

RENECKER, L.W., SILVERSIDES, D.W., PATEL, K. and OVERBEEK, P.A. (1995). TGFα can act as a chemoattractant to perioptic mesenchymal cells in developing mouse eyes. *Development 121:* 1669-1680.

ROCHETTE-EGLY, C., GAUB, M.P., LUTZ, Y., ALI, S., SCHEUER, I. and CHAMBON, P. (1992). Retinoic acid receptor beta: immunodetection and phosphorylation on tyrosine residues. *Mol. Endocrinol. 6:* 2197-2209.

ROCHETTE-EGLY, C., LUTZ, Y., SAUNDERS, M., SCHEUER, I., GAUB, M.P. and CHAMBON, P. (1991). Retinoic acid receptor gamma: specific immunodetection and phosphorylation. *J. Cell Biol. 115:* 535-545.

RUBERTE, E., DOLLÉ, P., CHAMBON, P. and MORRISS-KAY, G. (1991). Retinoic acid receptors and cellular retinoid binding proteins. II. Their differential pattern of transcription during early morphogenesis in mouse embryos. *Development 111:* 45-60.

RUBERTE, E., DOLLÉ, P., KRUST, A., ZELENT, A., MORRISS-KAY, G. and CHAMBON, P. (1990). Specific spatial and temporal distribution of retinoic acid receptor gamma transcripts during mouse embryogenesis. *Development 108:* 213-222.

RUBERTE, E., FRIEDERICH, V., CHAMBON, P. and MORRISS-KAY, G. (1993). Retinoic acid receptor and cellular retinoid binding proteins. III. Their differential transcript distribution during mouse nervous system development. *Development 118:* 267-282.

SEEWALDT, V.L., JOHNSON, B.S., PARKER, M.B., COLLINS, S.J. and SWISSHELM, K. (1995). Expression of retinoic acid receptor β mediates retinoic acid-induced growth arrest and apoptosis in breast cancer cells. *Cell Growth Differ. 6:* 1077-1088.

SHEN, S., VAN DER SAAG, P.T. and KRUIJER, W. (1993). Dominant negative retinoic acid receptor β. *Mech. Dev. 40:* 177-189.

SI, S.P., LEE, X., TSOU, H.C., BUCHSBAUM, R., TIBADUIZA, E. and PEACOCKE, M. (1996). RARβ2 mediated growth inhibition in HeLa cells. *Exp. Cell Res. 223:* 102-111.

TANEJA, R., ROY, B., PLASSAT, J.L., ZUSI, F.C., OSTROWSKI, J., RECZEK, P.R. and CHAMBON, P. (1996). Cell-type and promoter-context dependent retinoic acid receptor (RAR) redundancies for RARβ2 and Hoxa-1 activation in F9 and P19 cells can be artefactually generated by gene knockouts. *Proc. Natl. Acad. Sci. USA 93:* 6197-6202.

THOMAS, J.H. (1993). Thinking about genetic redundancy *Trends Genet. 9:* 395-399.

TRABOULSI, E. (1993). The eye. In *Human Malformations and Related Anomalies*, Vol. 2 (Eds. R.E. Stevenson, J.G. Halland and R.M. Goodman). Oxford University Press, New York, pp. 163-191.

UNDERWOOD, B.A. and ARTHUR, P. (1996). The contribution of vitamin A to public health. *FASEB J. 10:* 1040-1048.

VAN DER LEEDE, B.J., FOLKERS, G.E., KRUYT, F.A. and VAN DER SAAG, P.T. (1992). Genomic organization of the human retinoic acid receptor beta 2. *Biochem. Biophys. Res. Commun. 188:* 695-702.

WANEK, N., MUNEOKA, K., HOLLER-DINSMORE, G., BURTON, R. and BRYANT, S.V. (1989). A staging system for mouse limb development. *J. Exp. Zool. 249:* 41-49.

WARKANY, J. and SHRAFFENBERGER, S. (1946). Congenital malformations induced in rats be maternal vitamin-A deficiency. I. Defects of the eye. *Arch. Ophthalmol. 35:* 150-169.

WILSON, J.G., ROTH, C.B. and WARKANY, J. (1953). An analysis of the syndrome of malformations induced by maternal vitamin A deficiency. Effects of restoration of vitamin A at various times during gestation. *Am. J. Anat. 92:* 189-217.

WOLBACH, S.B., and HOWE, P.R. (1925). Tissue changes following deprivation of fat-soluble A vitamin. *J. Exp. Med. 42:* 753-777.

ZELENT, A., MENDELSOHN, C., KASTNER, P., KRUST, A., GARNIER, J.M., RUFFENACH, F., LEROY, P. and CHAMBON, P. (1991). Differentially expressed isoforms of the mouse retinoic acid receptor beta generated by usage of two promoters and alternative splicing. *EMBO J. 10:* 71-81.

ZHAO, D., McCAFFERY, P., IVINS, K.J., NEVE, R.L., HOGAN, P., CHIN, W.W. and DRÄGER, U.C. (1996). Molecular identification of a major retinoic-acid-synthesizing enzyme, a retinaldehyde specific dehydrogenase. *Eur. J. Biochem. 240:* 15-22.

ZOU, H. and NISWANDER, L. (1996). Requirement of BMP signaling in interdigital apoptosis and scale formation. *Science 272:* 738-741.

Received: February 1997
Accepted for publication: March 1997